TNO innovation for life

Geochemical characterisation of the Watervliet Member and groundwater in Paleogene and other sandy units of Zeeland

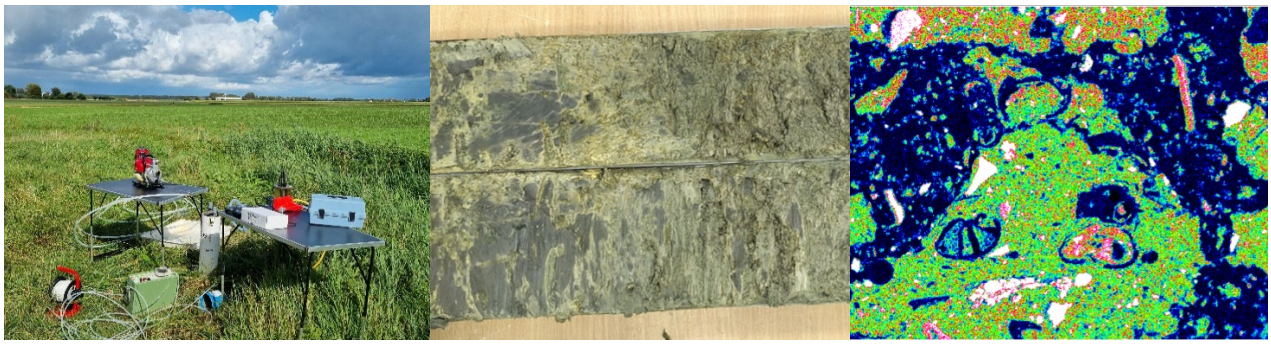

TNO Intern ⟩ TNO 2024 R12632
18 December 2024

Energy & Materials Transition
www.tno.nl
+31 88 866 42 56
info@tno.nl

TNO 2024 R12632 – 18 December 2024

Geochemical characterisation of the Watervliet Member and groundwater in Paleogene and other sandy units of Zeeland

Author(s) Alwina Hoving
Tano Kivits
Jasper Griffioen
supported by the geochemical laboratory of the Geo-Faculty of Utrecht University

Classification report	TNO Intern
Title	TNO Intern
Report text	TNO Intern
Appendices	TNO Intern
Number of pages	63 (excl. front and back cover)
Number of appendices	2
Sponsor	Ministerie van Infrastructuur en Waterstaat
Project name	Covra; Karakteriseren van Watervliet Klei
Project number	060.61501

Samenvatting/Summary

Samenvatting
Geologische berging wordt in Nederland beschouwd als één van de mogelijke beheeropties voor de eindberging van radioactief afval. Kleilagen zijn hierbij één van de opties waarbij de kleilaag als een natuurlijke, reactieve barrière functioneert. Na duizenden jaren of langer kunnen er radioactieve elementen uit het afval naar dit gastgesteente migreren. Inzicht in de geochemische eigenschappen van de kleilagen is daarom nodig. Uitgangspunt is dat het geochemische gedrag van een radioactieve element gelijk is aan het gedrag van datzelfde, stabiele element en dat sommige natuurlijk voorkomende, stabiele elementen geochemisch vergelijkbaar gedrag vertonen met radioactieve elementen. Dit wordt in het Engels aangeduid met het begrip ‘’natural analogues’’ ofwel in het Nederlands ‘’natuurlijke analogieën’’.

Voor Nederland gaat de aandacht uit naar de Paleogene kleilagen als gastgesteente. Eén van deze kleilagen is het Laagpakket van Watervliet dat ook wel wordt aangeduid als de Watervliet Klei. Deze studie presenteert: 1. een geochemische en mineralogische karakterisering van 24 sedimentmonsters van het Laagpakket van Watervliet zoals over de volledige diepte aanwezig in een boring uit Borsele en 2. een hydrochemische karakterisering van 15 grondwatermonsters uit zandlagen van Paleogene en jongere ouderdom zoals aanwezig in het midden en zuiden van Zeeland. Zeven sporenelementen zijn nader bestudeerd vanwege de radioisotopen die zich hiervan voordoen (Se, U, Th, Cs, Rn) of een natuurlijke analoog hiervoor zijn (Re, Eu of meer algemeen de zeldzame aardelementen).

De oorspronkelijk anoxische sedimentmonsters zijn afkomstig van een steekboring uit 2011 en waren inmiddels geoxideerd. Het analysepakket hield hier rekening mee. De mineralogie en geochemische samenstelling zijn bestudeerd aan de hand van bulk-analyses aangevuld met electronenmicroscopie. Het laagpakket vertoont een afwisseling van kleiige en zandige lagen in de 25 m die bestudeerd is: de ene helft van de monsters is klei en de andere helft zand of silt. De bovenste monsters zijn kalkrijk en kalk is afwezig in de onderste 15 m. De mineralogie wordt gedomineerd door kwarts, kleimineralen, veldspaten en calciet. Glauconiet komt ook veel voor. De gehalten van de nader bestudeerde sporenelementen zijn: U is 2 ± 0,9 ppm, Th is 7 ± 2 ppm, Se is 1 ± 0,3 ppm, Cs is 5 ± 2 ppm, Lu is 0,22 ± 0,05 ppm en Re is 7 ± 3 ppb. Deze waarden zijn vergelijkbaar met die in kleirijke geologische eenheden zoals de Boomse Klei in België en Nederland, alhoewel de gehalten gemiddeld iets lager liggen. Dit is waarschijnlijk te wijten is aan de aanwezigheid van zandige lagen in het bemonsterde laagpakket. De elementen U, Th, Cs en Se samen met de zeldzame aardelementen correleerden met de kleimineralen. Uranium en Se vertoonden ook een correlatie met pyriet. De gehalten van deze elementen zijn gemiddeld iets lager dan die in de Belgische of Nederlandse, Paleogene Boom Klei. Het verschil wordt verklaard door het zandigere karakter van het bestudeerde laagpakket in de boring. De waargenomen afwisseling van klei versus silt en zand is een aandachtspunt in relatie tot de functionele eigenschappen van het laagpakket of ingelegen kleilagen als gastgesteente. Zoals aangegeven in de stratigrafische nomenclator, is de afwisseling van zand- en kleipakketten een algemene, lithologische eigenschap van het Laagpakket van Watervliet.

Voor de grondwatermonsters zijn twee groepen te onderscheiden: 7 monsters komen uit diepe, begraven Paleogene aquifers met zoet tot zout grondwater van waarschijnlijk Pleistocene ouderdom en geïnfiltreerd in België of nabij de landsgrens. Acht monsters zijn afkomstig van ondiepe aquifers met zoet of zeer zout grondwater dat in het Holoceen zal zijn geïnfiltreerd. De monsters zijn altijd pH neutraal en kalkverzadigd en meestal anoxisch.

Antropogene verontreiniging van het bemonsterde grondwater is onwaarschijnlijk met uitzondering van de ondiepste zoete grondwatermonsters. Radon is als radioactief gas gemeten: de gemeten activiteiten liggen in het bereik dat typisch is voor Nederlands grondwater en zijn het hoogst voor monsters uit de begraven Tongeren Formatie. Voor de overige 6 elementen, zijn de concentraties in de ondiepe aquifers hoger dan in de diepe aquifers waarbij 1 diepe put wel uitschieters heeft voor U, Th en Eu. Selenium kent verreweg de hoogste concentraties tot 130 µg/l met geregeld concentraties boven de zeewater concentratie. De concentraties voor de overige 5 elementen liggen altijd onder 0,5 µg/l (behalve 1 uitschieter voor Th), hierbij ook onder de zeewater concentraties enkele uitzonderingen daargelaten en wel hoofdzakelijk boven de respectievelijke detectielimieten. Voor U en Se bestaan (inter)nationale drinkwaternormen en voor Eu is een indicatieve waarde afgeleid in de literatuur. Alle U en Eu concentraties liggen beneden deze waarden en voor Se in 5 ondiepe, zoute monsters erboven, de overige er onder. Voor het brakke en zoute grondwater kan vastlegging van U, Th, Re, Eu en Cs uit (verdund) zeewater zijn opgetreden en voor Se is juist mobilisatie opgetreden. Radon zal ondergronds van nature geproduceerd zijn. De rol van geochemische processen is niet verder herleid en is complex voor de redox-gevoelige elementen U, Se en Re, wat eenduidiger voor Th en Eu, en relatief eenvoudig voor Cs en Ra.

Deze studie zal als referentie dienen voor de geochemische en mineralogische samenstelling van het Paleogene Laagpakket van Watervliet en de samenstelling van grondwater met betrekking tot sporenelementen in Paleogene en jongere zandige pakketten in midden en zuidelijk Zeeland. De resultaten kunnen vergeleken worden met geochemische en mineralogische studies van andere Paleogene kleilagen en omringende watervoerende pakketten. Daarnaast kunnen de resultaten gebruikt worden voor risico-evaluaties van transport van radionucliden in grondwater.

Summary
In the Netherlands, geological disposal is considered as one of the future management options for the final disposal of radioactive waste. Argillaceous rocks are one of the options where these rocks act as natural reactive barriers. Radioisotopes may become released from stored waste in the course of hundreds to thousands or more years and migrate into these hostrocks. Insights in the geochemical properties of these rocks is therefore a necessity. Here, the geochemical behaviour of a radioactive element will be similar to its stable equivalent and some naturally occurring elements show geochemically identical behaviour to radioactive elements which is referred to as ''natural analogues''.

In the Netherlands, Paleogene clay layers are candidate hostrock for the final disposal of radioactive waste. One of these layers is the Watervliet Member which has also been referred to as the Watervliet Clay in literature. This study presents a geochemical and mineralogical characterisation of 24 sediment samples of this geological unit as fully present in a borehole drilled in Borsele (Zeeland) together with a hydrochemical characterisation of 15 groundwater samples from sandy layers from Paleogene and younger age as present in central and southern Zeeland. Seven trace elements get addressed in more detail for the existence of their radioisotopes (Se, U, Th, Cs and Rn) or being natural analogues for radioisotopes (Re, Eu or more generally rare-earth elements (REE)).

The originally anoxic sediment samples were taken out of sediment cores collected in 2011 and oxidised in the meanwhile. The set-up of the geochemical characterisation campaign took this oxidised status into account. The mineralogical and elemental, geochemical were performed on grab samples and scanning electron microcopy was performed on individual samples. The Watervliet Member showed an alternation of clayey and sandy/silty layers along the 25 meters of core samples. The upper samples were rich in carbonates and non-calcareous in the lower 15 meters. The mineralogy was dominated by quartz, clay minerals, feldspars and calcite. Glauconite was also frequently present. The contents of the trace elements of interest were on average: U is 2 ± 0.9 ppm, Th is 7 ± 2 ppm, Se is 1 ± 0.3 ppm, Cs is 5 ± 2 ppm, Lu is 0.22 ± 0.05 ppm and Re: 7 ± 3 ppb. These values are very similar to those in other clay formations such as the Boom Clay in Belgium and the Netherlands, although the values were slightly lower in the analysed Watervliet samples which is likely due to the sandy character of the sampled borehole. Uranium, Th, Cs and Se together with the REEs correlated to clay minerals. Uranium and Se also showed a correlation with pyrite. The total elemental contents were on average slightly lower than those in the Belgian or Dutch Paleogene Boom Clay. This difference is explained by the more sandy characteristic of the samples obtained from the borehole sampled. The observed alternation of clay versus silt or sand is a major point of attention in relation to the functional properties of the Watervliet Member or its clay layers as geological barrier. As described in the stratigraphic nomenclature, this alternation of clay and sand layers generally holds for the Watervliet Member.

Two compositional groups can be recognised for the set of groundwater samples: 7 samples were collected from deep, buried Paleogene aquifers containing fresh to saline groundwater from probably Pleistocene age and infiltrated in Belgium or near the national border. Eight samples were collected from shallow aquifers with either fresh or very saline groundwater from likely Holocene age. All samples are pH neutral and saturated for calcite and mostly anoxic. Anthropogenic contamination is unlikely given the hydrogeological settings except for the most shallow groundwater samples so the results serve as natural baseline. Radon was measured as radioactive gas: the radioactivity is typical for Dutch groundwater and highest for samples from the buried Tongeren Formation. The concentrations are higher in the shallow aquifers for the other 6 elements than in the deeper, buried aquifers except one deep well with outliers for U, Th and Eu. Selenium has by far the highest concentrations up to 130 µg/l with frequent exceedances of the seawater concentration. The concentrations for the other 5 elements were always below 0.5 µg/l

(except one outlier for Th) and also below the respective seawater concentrations except some exceptions but predominantly above the respective limits of quantification. Uranium and Se have (inter)national drinking water standards and an indicative value has been calculated in literature for Eu. All U and Se concentrations lie below these standards and 5 shallow, saline samples show exceedances for Se while the others lies below. For the brackish and saline groundwater, immobilisation of U, Th, Re, Eu and Cs from (diluted) sea water may have happened whereas geochemical mobilisation happened for Se. Radon gets produced in the subsurface. The geochemical controls have not been deduced any further and will be complex for the redox-sensitive elements U, Se and Re, slightly simpler for Th and Eu and relatively straightforward for Cs and Ra.

This study has resulted in a baseline study of the geochemical and mineralogical composition of the Paleogene Watervliet Member and trace elements composition of groundwater in Paleogene and younger sandy units in central and southern Zeeland. It will be useful as a reference for other Paleogene clay layers and surrounding sandy units and other purposes among which risk assessment for transport of radionuclides.

Contents

1 Introduction

The Dutch government announced that the preparations for the decision-making process on the final disposal of radioactive waste will start now. One of the steps to be taken is the disposal program where various types of final disposal will be considered. When it comes to subsurface disposal of radioactive waste, two types of geological deposits are generally considered in the Netherlands: Paleogene clay units and salt deposits. Geoscientific information about these deposits is needed in order to address the safety and sustainability of the geological disposal. For this reason research has been performed into these geological deposits as coordinated by COVRA, which is the organisation with the practical responsibility of sustainably handling Dutch radioactive waste, i.e., that collects, processes and stores all radioactive waste in the Netherlands. This work received funding from the Ministry of Infrastructure and Water Management.

There is a need for geochemical and mineralogical information on the Watervliet Member, which is a clay-rich deposit as part of the Paleogene Tongeren Formation (and coded as NMTOWA). Here, it is assumed that this layer can be found in various parts of the Netherlands at depths that are larger than where it is found in the province of Zeeland. The specific question is: what is the geochemical speciation of chemical elements in these clay-rich deposits in relation to the final disposal of radioactive waste? The Watervliet Member is the stratigraphic unit as presently recognised according to the Dutch nomenclature[1]. Earlier, the name ''Watervliet Clay'' was used, and the clay layer was characterised in the regional geohydrological model REGIS II v. 2.2 as first clayey unit of the Watervliet Bed and coded as TOZEWA-k1 (Zaadnoordijk et al., 2022).

In addition to sediment geochemical information on the geological units, there is also a need for hydrogeochemical information on the aquifers above or below this clayey unit. The related research question is whether or not the groundwater quality in these aquifers has been impacted by the clayey layers as aquitards. Primarily, we deal with sand layers in the Paleogene Tongeren and Rupel formations. Sand layers that are part of the Miocene Breda Formation also need attention as this formation directly lies on top of the Rupel Formation in southwestern Netherlands. Here, it will be part of the groundwater compartment that is directly fed by rain water and intrusion of sea water during more recent geological periods.

This report aims to present geochemical and mineralogical data on the Watervliet Member and hydrochemical data of Paleogene and other aquifers in the southern and central parts of the province of Zeeland. The analytical data was generated in the second part of 2024 by means of sampling and analytical campaigns organised by TNO Geological Survey of the Netherlands and supported by the geochemical laboratory of Utrecht University.

[1] https://www.dinoloket.nl/en/stratigraphic-nomenclature/by-stratigraphic-group/middle-north-sea-group/watervliet-member

2 Geology and hydrogeology

2.1 Hydrogeological structure

The geology in the upper few hundreds of meters is determined by Paleogene to Early Pleistocene marine formations that lie discordantly under shallow Early Pleistocene to Holocene formations (Figure 2.1). These formations may be fluvial, marine or periglacial.

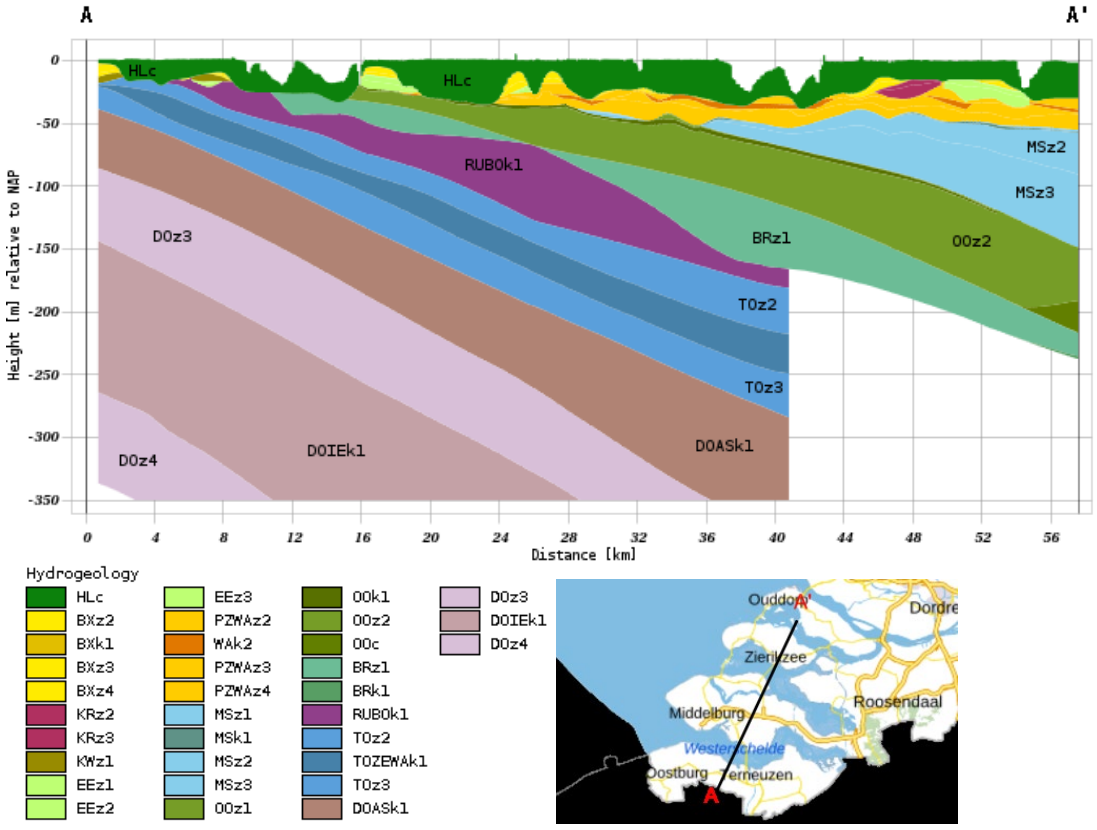

Figure 2.1: South-north geohydrological cross-section of the province of Zeeland according to REGIS II v2.2.2.

The Paleogene formations of Dongen (DO), Tongeren (TO) and Rupel (RU) slope downwards to the north from near the surface at Zeeuws-Vlaanderen to several hundreds of meters deep within a distance of tens of kilometers. These formations are composed of regional sandy and clayey layers. Note the presence of the TOZEWAk1 unit from the legend of Figure 2.1 which denotes the Watervliet Clay as geohydrological unit. The Watervliet Clay has been mapped for a part of Zeeland as indicated in Figure 2.2. The Neogene and Early Pleistocene marine formations of Breda (BR), Oosterhout (OO) and Maassluis (MS) are present near the surface further north and also slope downwards to the north. They are predominantly composed of sandy aquifers.

The younger formations are more horizontally oriented and they reach down to c. 50 m-NAP (NAP refers to Dutch ordnance datum) in the northern part. The Pleistocene deposits are predominantly sandy and the Holocene deposits are lithologically complex. The Peize-Waalre Formations (PZWA or WA) are not much present below the Western Scheldt and Zeeuws-Vlaanderen. The marine Eem Formation (EE) is discontinuously present as predominanly sandy layers in Zeeland. The fluvial Koewacht Formation (KW) originates from the Scheldt river system and is majorly present as sandy deposits in southern and eastern parts of Zeeland. The fluvial Kreftenheije Formation (KR) from the Rhine system is only present in the northern part of Zeeland and of minor interest for the current study. The periglacial Boxtel Formation is more or less discontinuously present and commonly sandy in this part of the Netherlands. The Holocene sediments reach down to 35 m-NAP and sometimes deeper under the Eastern or Western Scheldt. They are dominated by marine sediments with local peat layers.

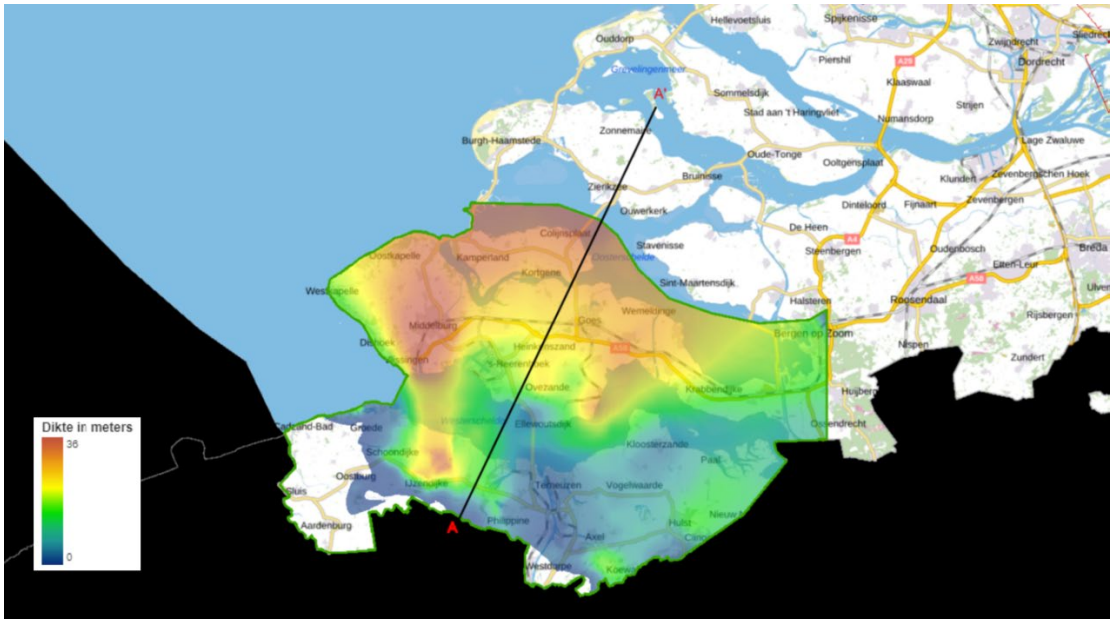

Figure 2.2: Thickness of the Watervliet Clay as mapped within the indicated area for the model REGIS II v2.2.2 model (www.dinoloket.nl).

Overall, the groundwater compartment above the Rupel Clay is predominantly composed of sandy marine sediments below the complex Holocene layer. This is highly relevant with respect to circulation of groundwater. The Paleogene aquifers are well separated from each other by rather thick regional clay layers which means they are hydraulically more isolated.

2.2 Groundwater dynamics

Data on groundwater heads can be found in the database of TNO Geological Survey of the Netherlands as accessible via www.dinoloket.nl. Table 2.1 summarises the already existing data on groundwater heads and Cl concentration (as indicator for salinity) for wells that were sampled within the framework of this project (see Chapter 3).

Wells that contain saline groundwater should be corrected for the difference in density between fresh and saline groundwater when the groundwater heads are intercompared. Seawater having a Cl-concentration of c. 19,000 mg/l has a density of 1.027 kg/L at 10°C while fresh water has a density of 0.99977 kg/dm^3 at 10°C (yearly average Dutch temperature of shallow groundwater). The correction is thus 2.7 cm per 1.00 m of water column for seawater. Five well screens show Cl concentrations around half that of seawater up to seawater and three of these have screen depths of 15 to 40 m-NAP. For observed heads around 0 m+NAP and a water column of 40 m, the correction would be 0.54 m when the Cl concentration is half that of seawater. This is substantial but does not lead to other insights in the regional hyrogeology.

Four groups of wells can be recognised based on the groundwater heads. First, three deep wells at Zeeuws-Vlaanderen show groundwater heads several meters below 0 m+NAP that generally decreased during 10 or more years. The associated salinity as based on Cl concentration is fresh to brackish. Second, two other deep wells at Zeeuws-Vlaanderen show groundwater heads around -1.0 n+NAP and contain brackish groundwater. For these groundwater heads, there is a gradual decrease of about 1 m in the course of c. 20 years. Third, two deep wells at Zuid-Beveland having brackish groundwater show groundwater heads close to 1.0 m+NAP without steady decrease in the course of 15-20 years. As salinity is fresh to brackish for these three groups, no density correction is needed for the heads. Last, eight wells at both Zeeuws-Vlaanderen and Zuid-Beveland that are shallow and vary in salinity from fresh to saline show groundwater heads near to 0 m+NAP. The correction for salinity may be up to 1 m for the well screens at 27-40 m-NAP when saline groundwater is present.

The Eocene aquifers have been studied in Flanders where they are locally referred to as Ledo-Paniselian and Ypresian Sands (Coetsiers et al., 2009). These sands refer to sand aquifers equivalent to the Dutch Dongen Formation. One may note that the Paniselian has fallen into disuse as chronostratigraphic term in Belgium (Vandenberghe et al., 2012) but still in use among Flemish hydrogeologists. The Ledo-Paniselian Sands are unconfined in the south and become semi-confined northwards. Groundwater is also recharged in the south by infiltration through the Bartonian Clay (equivalent to the Asse Member as part of the Dongen Formation) and important groundwater abstractions are present at Ghent and Sint-Niklaas. This may also explain the observed drawdown several meters below NAP in the aquifers of the Dongen Formation in Zeeuws-Vlaanderen. Hydrochemically, a sequence in water types is encountered from south to north: first fresh Ca-HCO_3 type (or Ca-SO_4 due to enhanced pyrite oxidation), next Mg-HCO_3, Na-HCO_3 and finally brackish Na-Cl type. The second and third water type are the result of freshening marine aquifers during which Ca from fresh water is exchanged for Na and Mg from seawater that is diluted or not.

Blaser et al. (2010) studied the groundwater age of a sample from the Dongen aquifer at well B48C0196 together with samples from Flemish wells using carbon isotopes and other tracers. They calculated a groundwater age of 41,190 ± 6,042 y for that well as based on ^{14}C modelling. Schout et al. (2024) sampled groundwater from the Tongeren aquifer at wells B48E0224 and B54F0093 (that were also sampled within the framework of the current project) and analysed for radioactive carbon amongst others. They found apparent ^{14}C ages around 35,000 y and did not make corrections to true age. The true age will likely be younger as ^{14}C is probably diluted by so-called dead carbon from degradation of sedimentary organic matter and/or dissolution of carbonates from Middle Pleistocene or older age. Schout et al. (2024) also analysed for $\delta^{37}Cl$ which indicates the ratio between the stable Cl isotopes ^{35}Cl and ^{37}Cl and its deviation from the seawater ratio. A value of 0.0‰ represents the seawater ratio and negative values are indicative for occurrence of diffusive transport in addition to advective transport for the current geoscientific settings (Beekman et al., 2011). The two samples from the buried Tongeren aquifer have values of -1.63‰ and -2.08‰ which indicates that transport of Cl has been diffusion controlled at some stage. This may be diffusion in the surrounding clay layers towards the aquifer or diffusion in the aquifer itself if groundwater has been stagnant.

Table 2-1: Summary of groundwater data as present in the on-line database Dinoloket operated by TNO Geological Survey of the Netherlands. The numbers for the groundwater heads were visually read from graphs. Chloride concentrations in brackets refer to outliers within a small series of hydrochemical analyses.

Well (+ screen no.)	Region	Formation	Cl concentration	gw head (at present)	top _screen	bottom _screen	summary
			mg/l	m+NAP	m+NAP	m+NAP	
B48C0196	Zeeuws-Vla.	Dongen	1977	-4.4	-119.21	-189.21	decrease from -3.2 m+NAP in 1996 to -4.3 m in 2013. About constant since then.
B55A0340	Zeeuws-Vla.	Dongen	87 - 149	-6.4 (in 2017)	-152.59	-205.99	decline from -6.0 to -7.8 m+NAP between 1996 and 2008, gradual increase to -7.2 m+NAP in 2016 and jump to -6.4 m+NAP in 2017
B55A0341	Zeeuws-Vla.	Tongeren	2500 - 2646	around -3.3 (in 2017)	-74.09	-101.09	around -2.3 m+NAP between 1996 - 2003 and gradual decrease since down to -3.3 m+NAP in 2017
B48H0291	Zeeuws-Vla.	Tongeren	980	around -1.0	-93.17	-149.27	after short increase from -0.4 m +NAP, gradual decrease from -0.2 to -1.0 m+NAP from 1996 to present
B54F0093	Zeeuws-Vla.	Tongeren	440 - 450	around -0.8	-75.44	-145.44	gradual decrease from around 0 m+NAP in 2000 to -0.9 m+NAP in 2021 with amplitude of 0.6 m
B48E0224	Zuid-Bev.	Tongeren	2000	1.15 to 1.3	-126.3	-131.3	fluctuations between 1.1 and 1.3 m+NAP from 2005 to present
B48G0204	Zuid-Bev.	Tongeren	460 - 689	0.8 to 1.1	-89.78	-147.78	increase from 0.7 to 1.0 m+NAP between 1996 - 2001. Fluctuation around 1.0 m from 2008 to present
B54B0093	Zeeuws-Vla.	Tongeren	-	around 0.2	-16.48	-17.48	fluctuations between -0.5 to 1.0 m+NAP from 2006 to present
B54E0238-001	Zeeuws-Vla.	Holocene	7315 - 12697	around 0.1 (in 2001)	-1.1	-2.1	fluctuations between -0.6 to 0.5 m+NAP between 1988 to 2001
B54E0238-002	Zeeuws-Vla.	Boxtel	10900 - 12116 (19885)	around 0.1 (in 2001)	-5.07	-6.07	fluctuations between -0.6 to 0.6 m+NAP from 1988 to 2001
B54E0238-003	Zeeuws-Vla.	Tongeren	12195 - 13833	around 0.1 (in 2001)	-20.45	-21.45	fluctuations between -0.6 to 0.6 m+NAP from 1988 to 2001 (comparable to filter 002)
B48G0100-001	Zuid-Bev.	Holocene	13 - 120 (1035)	around -0.4	-2.78	-3.78	fluctuations between -0.9 and 0.3 m+NAP from 1991 to present
B48G0100-004	Zuid-Bev.	Holocene	56 - 1395	around -0.4	-16.89	-17.89	comparable to filter 001
B48G0100-005	Zuid-Bev.	Waalre	1666 - 18847	around -0.6	-27.75	-28.75	fluctuations between -0.9 and 0.1 m+NAP during 1991 - 2006 and decrease to fluctuations between -1.2 to -0.2 m+NAP since until present
B48G0100-006	Zuid-Bev.	Breda	9300 - 20180	around -0.7	-39.92	-40.92	fluctuations between -1.3 and 0 m+NAP from 1991 to present

3 Methods

3.1 Sediment

3.1.1 Sediment cores

TNO received 24 cores from borehole KB101. KB101 was drilled in 2011 at COVRA (Borsele; PCR, 2013). Large intervals of this drilling were cored. Directly after drilling, the PVC liners of these cores had been cut open and the sediment was lithologically described. After this the two halves had been put back together and stored in another PVC liner with a larger diameter (Figure 3.1). Since 2011, these cores were stored under ambient conditions at COVRA. In this borehole, the sediment of interest for this study, the Watervliet Member, is present from 95-118 meters below surface (MBS). The interval 95-97 MBS is on the boundary Ruisbroek Sand-Watervliet Member.

Figure 3.1: Example of a sediment core as received. Top: outer liner. Middle: original liner that had already been opened in the past. Bottom: Reopened liner with brown colour as a clear sign of oxidation.

The first core was (re)opened in a glovebag under N_2 atmosphere to ensure that the sediment would not oxidize before analysis. However, upon opening it was clear from the brown/red/yellow color of the sediments and presence of gypsum crystals that the cores were already oxidized and dried-out due to the long storage times in the PVC liners (see Figure 3.1 and Appendix A). Therefore, the other cores were not opened and sampled in a glovebox. From each core, the top 2 cm was stripped-off to remove the material that was most oxidized. The middle of the core was sampled, lithologically described, and then freeze-dried. A subsample was ground in an agate mortar after which it was used for major, minor, and trace elements analysis by X-Ray Fluorescence (XRF, Thermo ARL 9400 sequential XRF). Major elements were measured on a fusion bead while trace elements were measured on a pressed pellet. Total carbon (C_{total}), organic carbon (C_{org}) and sulfur content were

analyzed by combustion and infrared detection (Leco SC632). Thermogravimetric analysis was carried out to assess organic matter content and carbonate content (Leco TGA701). Not all trace elements of interest can be analyzed by XRF. Therefore the sample was also analyzed by Inductively Coupled Plasma-Mass Spectroscopy (ICP-MS, PerkinElmer NEXION 2000P) after dissolving the sediment in an HF-HNO_3-$HClO_4$ solution.

Mineralogy was analyzed by X-Ray Diffraction (XRD, Bruker D8 Advance with DAVINCI). For quantitative mineral analysis of the bulk samples, corund was added as an internal standard. Clay mineralogy was analyzed using the method described by Zeelmaekers (2011)

A sequential extraction was carried out to analyze to which mineral or substance the trace elements are associated. The sequential extraction consisted of 4 steps targeting 1. Exchangeable ions (1 M $MgCl_2$ solution), 2. Carbonates (1 M Na-acetate/acetic acid pH 4.5), 3. Organic matter (0.7M Na-hypochlorite), 4. Fe/Mn-oxides (0.2M oxalate/oxalic acid) (Gleyzes et al., 2002). Solely step 3 targeting organic matter was analyzed with ICP-MS, since trace elements in other minerals will be analyzed with LA-ICP-MS. In addition, a few characteristic samples were analyzed by Scanning Electron Microscopy with energy dispersive X-ray spectroscopy (SEM-EDX) to see whether some trace elements are specifically present in certain minerals. However, the detection limit of SEM-EDX could be too high for certain trace elements of interest. For this, the samples were embedded in epoxy of which polished thin sections were made.

3.2 Groundwater

3.2.1 Well selection & sampling

To get an idea of the influence of the Watervliet Member on surrounding aquifers, multiple groundwater wells were selected for sampling. The wells were selected based on the proximity of the filters to the Watervliet Member in the Tongeren Formation. In total, ten groundwater wells were sampled, all in the province of Zeeland (see Figure 3.2) due to the occurrence of the Tongeren Formation in that province. Seven of the ten wells have filters in the Tongeren Formation near the Watervliet Member and two are situated in the deeper Dongen Formation (see Figure 3.3 and Table 3.1). Two multi-level wells were also selected to be sampled (B48G0100 and B54E0238) with the goal of sampling shallower formations, in order to collect data from the near the surface on.

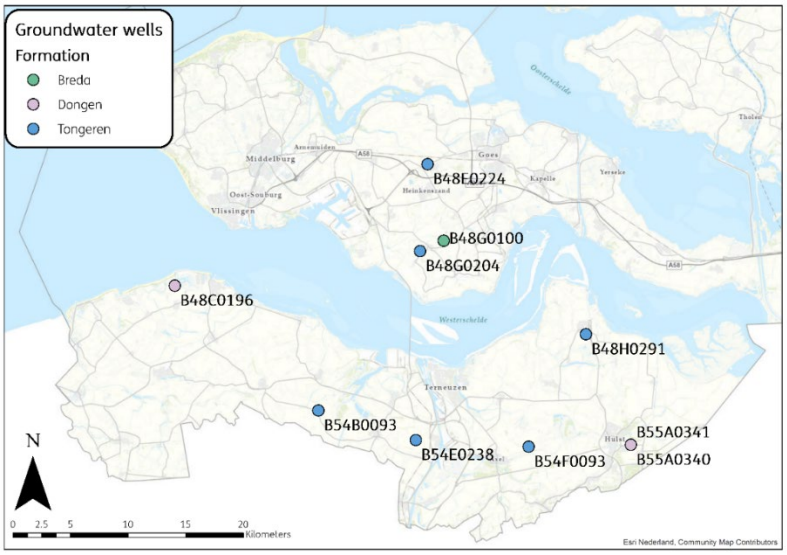

Figure 3.3: Map of the locations of the groundwater wells. The colour indicates the deepest formation that the well reaches. The symbols for B55A0340 and B55A0431 overlap, these wells are situated next to each other with one reaching the Tongeren Formation and the other reaching the Dongen Formation. B48G0100 and B53E0238 are multi-level wellls with multiple filters above the formation with is indicated here

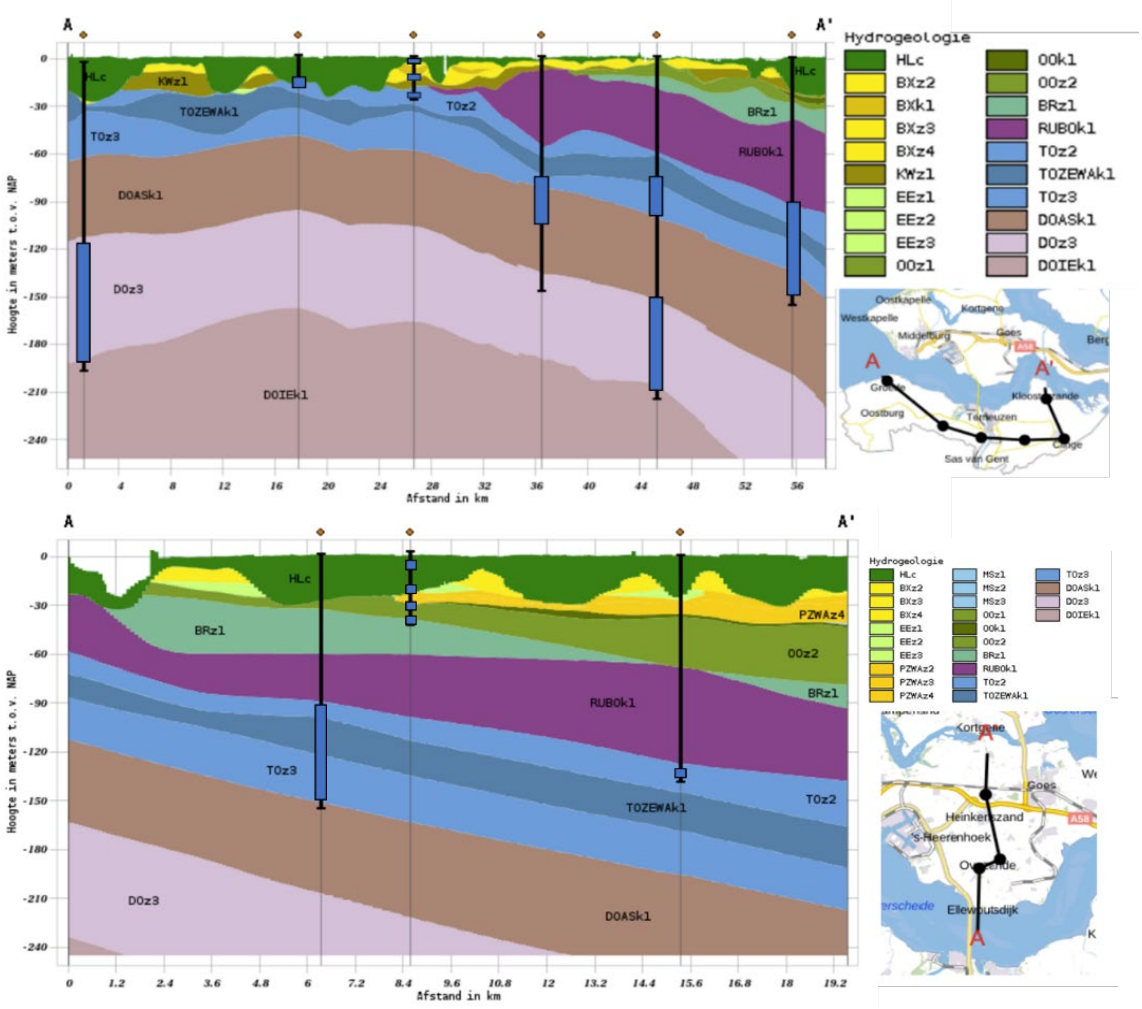

Figure 3.2: Profiles through REGIS II showing the filter depths (blue bars) of the sampled wells

Originally, the plan was to sample several filters of well B48H0124 near 's-Gravenpolder instead of B54E0238, but during the fieldwork it turned out that the deepest filters of this well were glued shut and could not be opened. Therefore, this well was substituted with the multi-level well B54E0238 and an additional filter in the Tongeren Formation (B54B0093). It was originally also planned to sample well B55A0364 near Graauw, but the well had a kink at ca. 6.5 meter below surface (mbs) which made sampling impossible. Furthermore, well B54F0093 has an additional deeper filter in the Dongen Formation next to the sampled filter in the Tongeren Formation. Unfortunately this deeper filter could not be sampled due to the deep hydraulic head in this well (8.5 mbs) which made pumping impossible.

Table 3-1: Overview of the sampled wells with well codes, filter numbers, locations, sample dates, the measured hydraulic heads, the depth range of the filters and the formation that the filters are situated in.

Sample name	Well code	Filter	Location	Sample date	Hydraulic head (mbs)	Top of filter (mbs)	Bottom of filter (mbs)	Formation
WV01	B48G0100	1	Ovezande	3-9-2024	3.36	5.6	6.6	Holocene
WV02	B48G0100	4	Ovezande	3-9-2024	3.35	19.7	20.7	Holocene
WV03	B48G0100	5	Ovezande	3-9-2024	3.37	30.5	31.5	Peize/Waalre
WV04	B48G0100	6	Ovezande	3-9-2024	3.66	42.7	43.7	Breda
WV05	B48G0204	1	Ovezande	4-9-2024	-0.05	90.9	148.2	Tongeren
WV06	B48E0224	1	's-Heer Arendskerke	4-9-2024	-0.05	127.5	132.5	Tongeren
WV07	B55A0340	1	Hulst	4-9-2024	7.48	153.8	207.15	Dongen
WV08	B55A0341	1	Hulst	5-9-2024	6.35	75.15	102.15	Tongeren
WV09	B48C0196	1	Groede	10-9-2024	2.41	117	187	Dongen
WV10	B54E0238	1	Sluiskil	10-9-2024	1.87	2.6	3.6	Holocene
WV11	B54E0238	2	Sluiskil	10-9-2024	1.92	6.5	7.5	Boxtel
WV12	B54E0238	3	Sluiskil	10-9-2024	1.9	21.9	22.9	Tongeren
WV13	B54B0093	1	Pyramide (IJzendijke)	10-9-2024	2.27	18.4	19.4	Tongeren
WV14	B48H0291	1	Kloosterzande	11-9-2024	1.84	93.9	150	Tongeren
WV15	B54F0093	1	Axel	11-9-2024	2.04	77	100	Tongeren

The wells were pumped using either a submersible pump (Grundfos MP1), a centrifugal pump (Honda WX10) or a peristaltic pump (Eijkelkamp), depending on the diameter of the well. Several of the sampled wells had very large diameters (15 cm, see Figure 3.4), which implied that large volumes of water had to be pumped (several thousands of liters). The wells were sampled after purging at least three times the water volume in the well, and when the field parameters (pH, electrical conductivity, temperature & dissolved oxygen) had reached stable values. The groundwater samples were always taken with either the submersible or peristaltic pump since the centrifugal pump is not suitable for taking good quality samples.

Figure 3.4: Well B48G0204 (Overzande), with a large well diameter of 15 cm.

After sampling wells B55A0340 and B55A0341, it was found that the numbering of the wells was possibly switched. These two wells are both situated at the waste water treatment plant of Hulst, at a distance of approximately 10 meters from each other (see Figure 3.5). These wells are described by a report from the University of Gent (Vermoortel et al., 1996). The wells were originally drilled for the purpose of carrying out pumping tests to see if groundwater could possibly be abstracted from deeper aquifers for drinking water production. The report includes a map of the drilling locations of the wells, where the well indicated “Hulst-Eoceen” is located south of “Hulst-Oligoceen”. “Hulst-Eoceen” is the deeper well of the two, reaching a depth of 216 m below surface. This should correspond with well B55A0340 in DINO, but the marking on the southern well says B55A0341 (see the right well of Figure 3.5). The report of the University of Gent also includes groundwater quality data, the results from sample WV7 match with the old data for “Hulst-Eoceen” and WV8 matched with “Hulst Oligoceen”, which indicates that the southern well should be B55A0340 instead of B55A0341 (see Table 3-2). Since this wrong numbering on the wells was discovered after sampling, the deeper well was pumped for a shorter time than planned. However, the volume of the well was still purged two times (instead of the more usual 3 times), and the field parameters were stable. Also, the new results match the old data, which gives confidence that the sample is of sufficient quality despite the shorter pumping time.

Figure 3.5: Wells B55A0340 and B55A341 at the wastewater treatment plant of Hulst. The photo is taken towards the east. The numbering on the wells indicate that B55A0340 is in the north, while B55A0341 is in the south. However, the map of Vermoortel et al. (1996) indicates that it should be the other way around.

Table 3-2: Comparison of the data for the wells “Hulst-Eoceen” and “Hulst-Oligoceen” from Vermoortel et al. (1996) and samples WV7 and WV8. Based on this comparison, it can confidently be concluded that sample WV7 is from the well in the Dongen Formation, and WV8 is from the Tongeren formation.

Parameter	Hulst-Eoceen	Sample WV7	Hulst-Oligoceen	Sample WV8
Na (mg/l)	1928	1770	367	358
K (mg/l)	37.9	35.7	14.2	14.2
Ca (mg/l)	38.7	29.3	5.71	3.8
Mg (mg/l)	23.7	24.1	3.5	3.3
Fe (mg/l)	0.2	0.2	0.74	0.1
Mn (mg/l)	0.07	0.02	0.09	0.2
Cl (mg/l)	2646	2604	149	140
SO_4 (mg/l)	163.8	148	22.23	6
NO_3 (mg/l)	0.24	0.09	1.1	0
Alkalinity (as HCO_3; mg/l)	691.74	780	688	927
EC (µS/cm)	6560	9100	1346	1532
pH (-)	7.93	8	8.59	8.85

3.2.2 Analytical methods & speciation calculations

pH, electrical conductivity, temperature and dissolved oxygen were all measured as field parameters using electrodes. The alkalinity was also determined in the field with a HACH digital titrator. For most samples, radon (Rn) was determined in the field using a Durridge RAD7 radon detector. Samples were taken for lab analysis with TIC-analysis, ion chromatography (IC), ICP-MS and ICP-OES by Utrecht University after filtration through a 0.45 µm micropore filter and acidified using HNO_3 for ICP-analysis. Here, the anions Cl, SO_4, Br, F, NO_3, NO_2 and ortho-PO_4 were analysed by IC. Aluminium (Al), B, Ca, K, Mg, Na, P, S, Si and Ti were analysed by ICP-OES where Ti was found to be commonly below the limit of quantification (being equal to three times the limit of detection). Barium (Ba), Be, Cd, Co, Cr, Cu, Fe, Li, Mn, Mo, Ni, Pb, Sc, Sr, V, Y, Zn and Zr were analysed by both ICP-OES and ICP-MS where the detection limits for ICP-MS are always lower. Silver (Ag), As, Ce, Cs, Dy, Er, Eu, Gd, Hf, Hg, Ho, La, Lu, Nb, Nd, Pr, Rb, Re, Sb, Se, Sm, Sn, Ta, Tb, Th, Tl, Tm, U, W and Yb were analysed by ICP-MS. Here, three elements were always found below their limits of quantification using ICP-MS: Nb, Ag and W. Four other elements were found three times or less above their limits of quantification: Be, Cd, Sn and Ta. The geochemical model code PHREEQC (Parkhurst & Appelo, 2013) was used to perform speciation calculations and calculate the saturation index (defined as the log-value of the ratio between the ion activity product and the solubility constant) with respect to minerals and other hydrochemical properties.

Additional samples were taken for the determination of dissolved methane (Isolab), ^{14}C (CIO, Groningen), ^{18}O, ^{2}H and ^{37}Cl (IPCP, Paris). The results for the isotope analyses were not yet available at the beginning of December 2024 and will be reported separately.

4 Results and Discussion

4.1 Sediment

4.1.1 Major elements and main mineralogy

The content of major, minor and trace elements in the samples measured by XRF and ICP-MS as well as C-S and TGA results can be found in Appendix A.1, A.2, A.3. Bulk mineralogical results and clay mineralogy are listed in Appendix A.4 and A.5.

A depth profile of silicium (Si), aluminium (Al), inorganic carbon (TIC) and organic carbon (C_{org}) is plotted together with lithology and main mineralogy from XRD in Figure 4.1. The samples from the trajectory studied are not all classified as clay, as may be suggested by the name ''Watervliet Clay'' that has been commonly used for these deposits. Instead, half of the samples in this trajectory is classified as clay, while the other half classifies as sand or silt. This is a main reason why the layer is indicated as ''Watervliet Member'' in this report. This is also in agreement with the current stratigraphy for Dutch geological deposits[2]. The Si content correlates very well with the quartz content, while the TIC content corresponds well with the calcite content. Calcite is mainly present between 98-105 mbs. The quartz content fluctuates greatly with depth varying with the alternating sandy, clayey and silty layers. Aluminium, which is a major element in clay minerals, but also in feldspars, is often in antiphase with Si/quartz and has the highest values in the clayey layers. The sulfur content, which correlates very well with pyrite, is highest at 97, 114,115 and 121 mbs. Organic carbon exhibits peaks at the same depths as calcite, but has extra peaks at 115 m and 120 m depth.

The bulk mineralogy is listed in Table 4-1. The sediment mainly consisted of quartz, 2:1 clay minerals (including mica and glauconite), feldspars, calcite and kaolinite. Low quantities (<1%) were present of ankerite, siderite, pyrite, clinopyroxene, rutile and anatase. Secondary minerals jarosite and gypsum were also present with maximum quantities of 5% and 2%, respectively. These secondary minerals can form upon oxidation of the cores and evaporation of the pore water. These two secondary minerals likely originate from the oxidation of pyrite. Oxidation of pyrite in the presence of carbonates, such as calcite, can lead to the formation of gypsum and Fe-(oxyhydr)oxides. Pyrite oxidation releases acidity which results in the dissolution of carbonates. If all carbonates are dissolved, the pH decreases and jarosite can form as an oxidation product. Assuming all S originates from pyrite, the original pyrite content of these sediments would have been on average 2.0% ± 1.6.

[2] https://www.dinoloket.nl/en/stratigraphic-nomenclature/watervliet-member

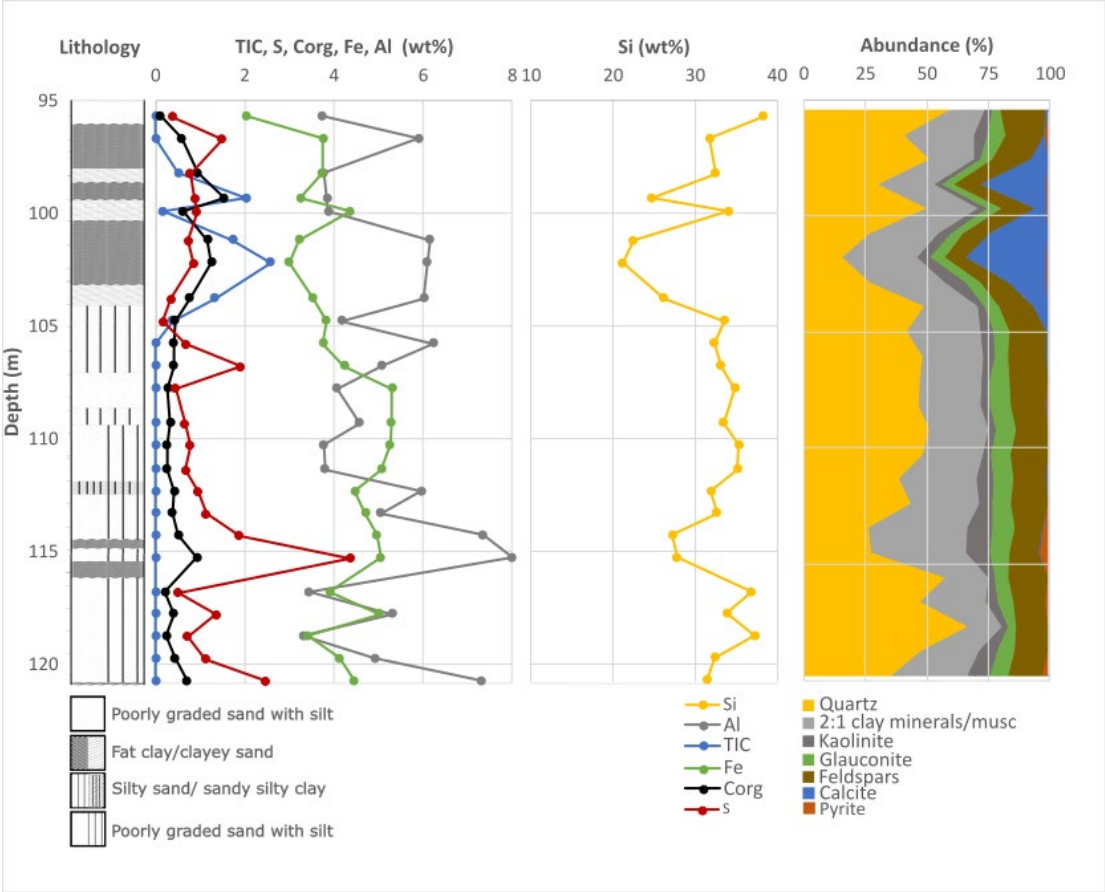

Figure 4.1: Depth profile of Watervliet Member at borehole KB101 with main lithology (left), total inorganic carbon (TIC), organic carbon (C_{org}), aluminium (Al), iron (Fe), and silicium (Si) content (middle), and main mineralogy (right).

Table 4-1: Summary of the mineralogy of the Watervliet Member samples.

Mineral	MIN (wt%)	MAX (wt%)
Quartz	13.5	60.5
2:1 clay minerals/ mica/glauconite	11.7	32.8
Kaolinite	2.2	8.2
Feldspars	7.5	19
Calcite	0.0	29.1
Ankerite	0.0	2.2
Pyrite	0.0	2.61
Rutile	0.5	1.37
Anatase	0.8	1.6
Clinopyroxene	0.4	2.3
Gypsum	0.1	2.2
Jarosite	0.0	4.8

4.1.2 SEM imaging and LA-ICP-MS

Scanning Electron Microscopy of the samples showed the predominant presence of rounded-angular quartz grains and clusters of clay minerals (see Figure 4.2). Pyrite was mostly present as small framboids of 5-10 µm with individual crystallites of 1 µm. Larger pyrite aggregates of 30 um were sporadically present. Rounded glauconite grains were also present as were large angular grains of rutile/anatase. Trace element analysis by energy dispersive X-ray spectroscopy (SEM-EDX) showed the presence of arsenic in pyrite and chromium in glauconite. Mapping of elements in sample KB101-100 (Figure 4.3) clearly visualized the different minerals such as quartz, calcite, mica, pyrite, rutile, feldspars and pyrite. The detection limit of SEM-EDX was too high for other trace elements of interest, such as REE, U or Se. Therefore the trace elements that are analogues for radionuclides will be further investigated by LA-ICP-MS.

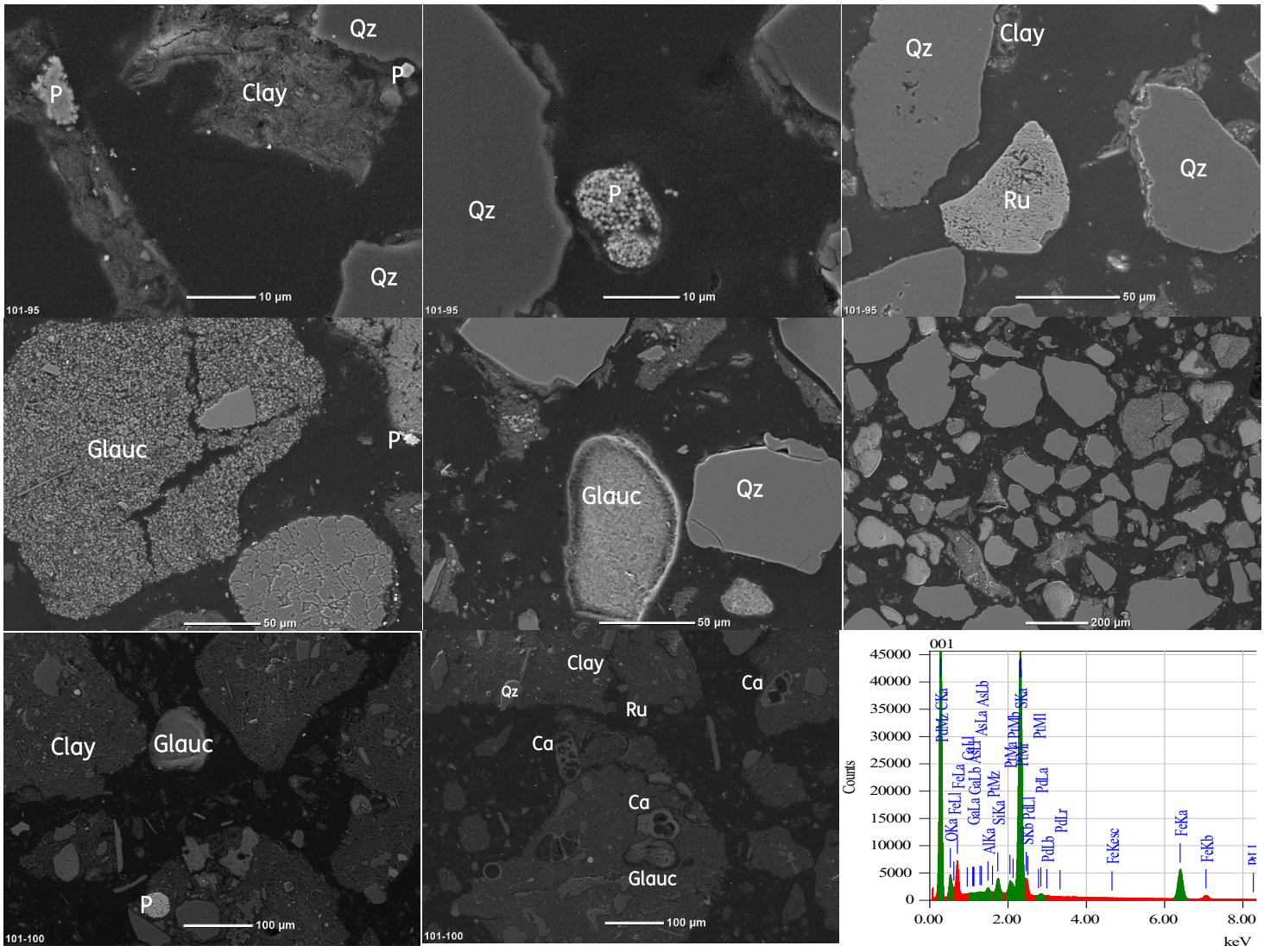

Figure 4.2: Scanning Electron Microscope images of samples KB101-95 (top) and KB101-116 (middle) and KB101-100 (bottom). Qz = quartz, Glauc = glauconite, P = pyrite, Ru = Rutile, Clay = clay minerals, Ca = calcite. Image on the lower right is an example of an EDX analysis of a pyrite grain.

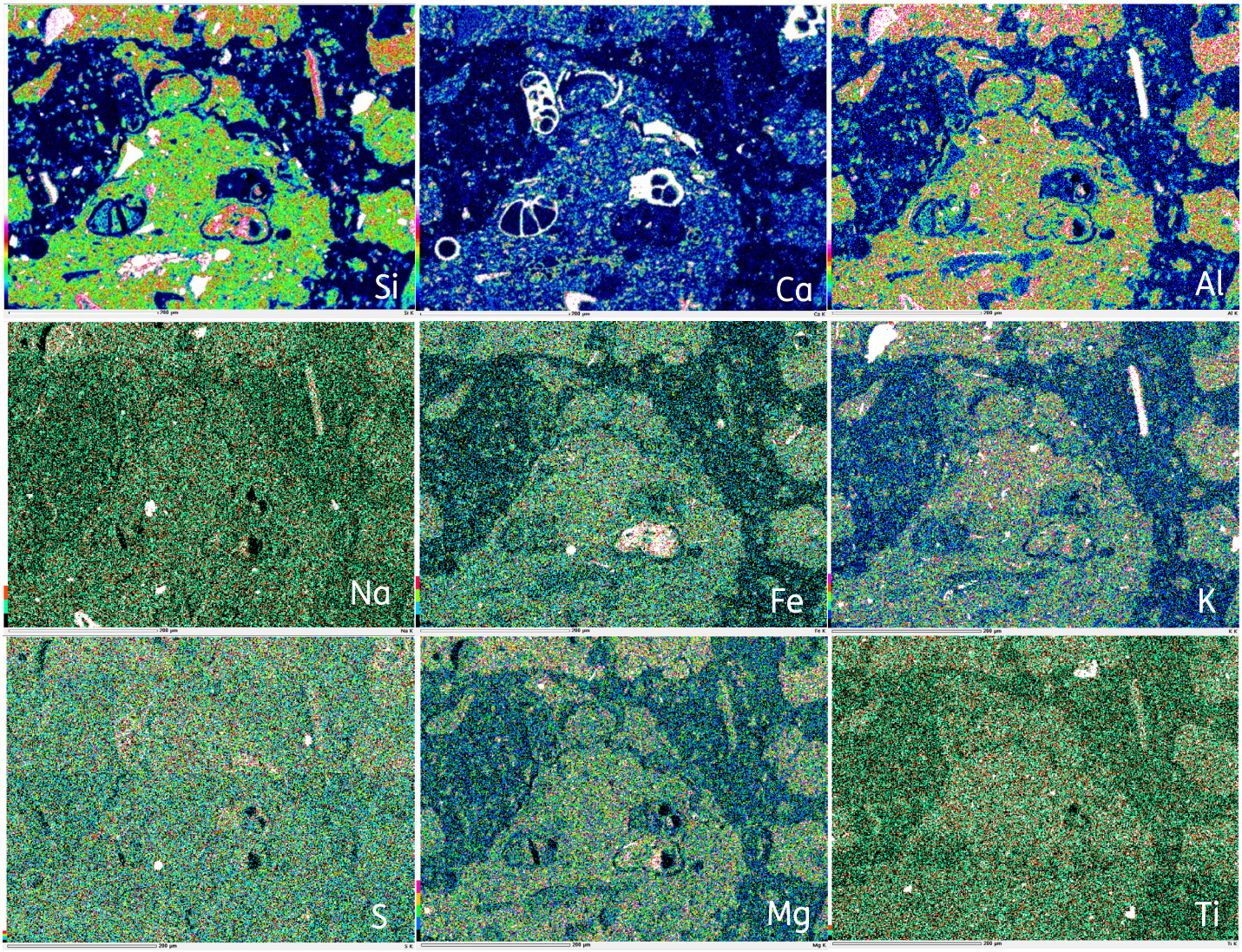

Figure 4.3: Scanning Electron Microscope images. Energy dispersive X-ray (EDX) elemental mapping of Si, Ca, Al, Na, Fe, K, S, Mg, and Ti in of sample KB101-100. Colours represent relative abundance of the element. Black indicates the element is below the detection limit, lowest counts are represented by dark blue, followed by turquoise, green, yellow, red, pink and white, which represent the highest counts.

4.1.3 Trace elements

All measured values of trace elemental content in the samples can be found in Appendix A. A few relevant trace elements that can be used as natural analogue for radionuclides in radioactive waste disposal are plotted in Figure 4.4. Uranium content is on average 2 ± 0.9 ppm, Th 7 ± 2 ppm, Se 1 ± 0.3 ppm, Cs 5 ± 2 ppm, Lu 0.22 ± 0.05 ppm and Re 7 ± 3 ppb. A depth profile of U, Th and Cs is plotted in Figure 4.5 as well as Al, organic C and S. All these elements have peaks at the same intervals. Correlations between trace elements and all other measured elements are presented in the correlation matrix (Figure 4.6). Based on the highest correlations between elements ($|R| > 0.6$), a few groups can be discerned as presented in Table 4.2. The Al content is positively correlated to Ti, Mg and a large group of trace elements. This group likely represents clay minerals. Titanium itself has a high correlation with Co and a very high correlation with the heavy rare earth elements (HREE: Gd to Lu). Ti-oxides are known to concentrate these elements (Hutchinson et al., 2001). A second group contains Fe, K, Cr and Be. The exact nature of this group is uncertain. Both glauconite and biotite contain Fe and K. Beryllium concentrations can be elevated in glauconite (Dooley, 2001). Chromium is well-known to be able to substitute Fe in Fe-bearing minerals. Although glauconite and biotite also contain Al, this correlation could be obscured by the presence of Al in other minerals. Group 3 and 4 correlate very well with calcite and quartz. Zircon is known to have Hf substituting for Zr, which comprises group 5. In the last group, S shows a positive correlation with As, V, Mo, U and Se. This group likely represents pyrite. The trace metals Mo and As are commonly pyritized in anoxic marine sediments (Raiswell and Plant 1980; Huerta-Diaz and Morse, 1992).

Table 4-2: Elemental groups that are recognised from the correlation matrix presented in Table 4.1.3.

Group	Elements in group	Associated mineral
Group 1	a. Al, Mg, Ti, Cu, Pb, Ni, Zn, Ga, Nb, Sc, **Th**, Li, **Se, Cs**, Ta, LREE, U b. Ti, Nb, HREE (Gd to Lu)	a. Clay minerals b. Ti-oxide
Group 2	Fe, K, Cr, Be	Glauconite/Biotite
Group 3	Ca, Mn, Sr	Calcite
Group 4	Si, Rh	Quartz
Group 5	Zr, Hf, Ag	Zircon
Group 6	S, As, V, Mo, U, Se	Pyrite

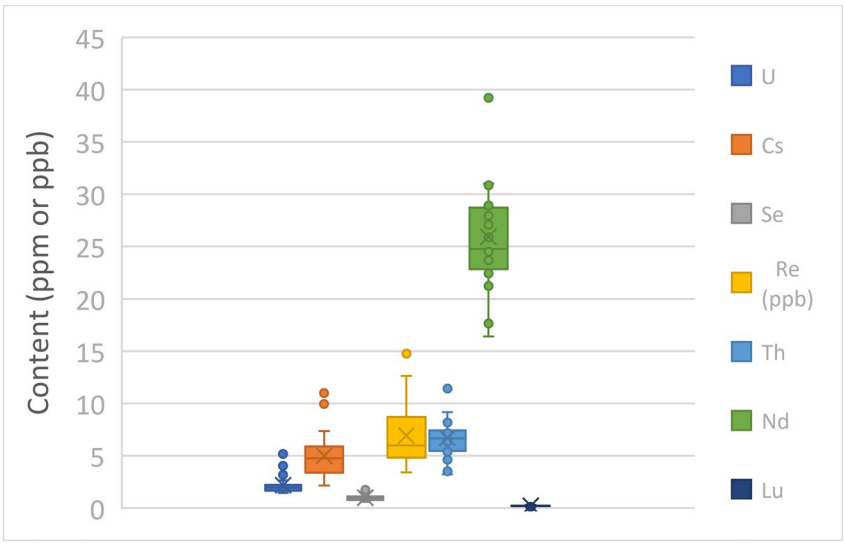

Figure 4.4: Box plots of the content of uranium, cesium, selenium, rhenium, thorium, neodymium and lutetium in samples KB101-95 to KB101-118.

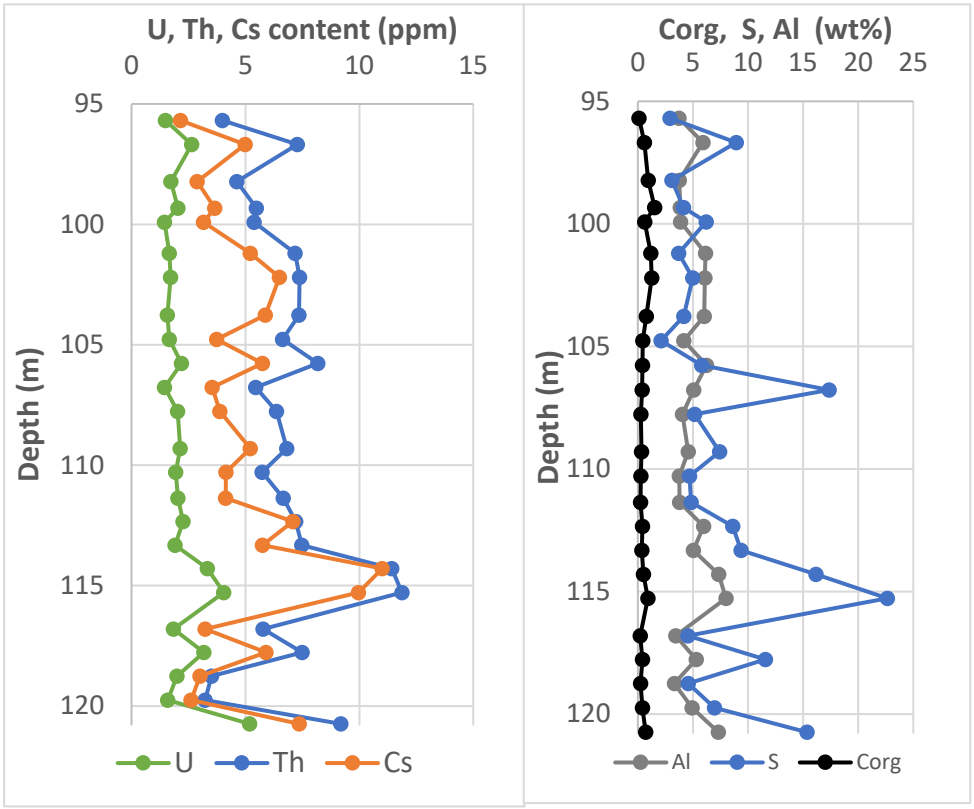

Figure 4.5: Depth profiles of U, Th and Cs (left), and organic carbon, sulfur and aluminium (right)

	Al	Ca	Fe	K	Mg	Mn	Na	P	Si	Ti	As	Cr	Cu-Ni-Pb	Hf	LREE	Rb	S	Sr	Th	U	V	Zn	Zr	Rh	Be	Cd	Co	Li	Mo	Se	Ag	Cs	HREE	Ta and Nb	Re
Al	1				0.77				-0.6	0.82	0.68		0.88		0.68	0.68	0.7		0.84	0.66	0.67	0.81						0.91		0.81		0.88	0.76	0.88	
Ca		1				0.88			-0.8									0.99																	
Fe			1	0.76								0.89				0.68					0.62				0.89										
K				1								0.77				0.61									0.8										
Mg					1					0.72			0.72		0.81	0.85			0.9		0.75	0.62					0.62	0.87		0.78		0.91	0.7	0.82	
Mn						1			-0.78									0.87																	
Na							1																												
P								1																											
Si									1															0.71											
Ti										1	0.6		0.83	0.61	0.73				0.85			0.82					0.76	0.8		0.78	0.63	0.77	0.91	0.9	
As											1		0.85		0.81	0.79	0.86		0.75	0.78	0.9	0.62						0.78		0.69		0.78	0.67	0.72	
Cr												1			0.7	0.82					0.78				0.95										
Cu-Ni-Pb													1		0.82	0.72	0.79		0.88	0.78	0.77	0.81					0.7	0.91		0.9		0.88	0.85	0.9	
Hf														1									0.98								0.96		0.62		
LREE															1	0.87	0.61		0.91	0.74	0.87	0.67			0.65		0.69	0.84		0.81		0.87	0.83	0.8	
Rb																1	0.67		0.87	0.7	0.96				0.8			0.85		0.66		0.9	0.61	0.7	
S																	1		0.67	0.7	0.72							0.75	0.81	0.64		0.69		0.67	
Sr																		1																	
Th																			1	0.71	0.83	0.74					0.67	0.94		0.86		0.94	0.85	0.89	
U																				1	0.74	0.64				0.69		0.74		0.75		0.7	0.63	0.61	0.76
V																					1				0.77			0.83		0.67		0.87	0.62	0.7	
Zn																						1					0.82	0.72		0.76		0.72	0.87	0.85	
Zr																							1								0.92				
Rh																								1											
Be																									1										
Cd																										1									0.76
Co																											1			0.76			0.84	0.8	
Li																												1		0.87		0.98	0.79	0.88	
Mo																													1						
Se																														1		0.84	0.83	0.86	
Ag																															1		0.67		
Cs																																1	0.79	0.88	
HREE																																	1	0.89	
Ta and Nb																																		1	
Re																																			1

Figure 4.6: Correlation matrix between geochemical parameters for the Watervliet Member in samples from KB101. Only values of |R| > 0.60 are shown.

4.1.4 Trace elements as natural analogue

The behaviour of radionuclides in a radioactive waste repository is often studied in laboratory experiments. However, these are relatively short-term compared to the lifetime of radioactive waste. An additional approach to predict radionuclide behaviour is by studying natural elements/radionuclides with analogue geochemical behaviour. This can be done by studying the same radionuclide directly like U and Th, or by studying stable isotopes of the same element, for example, Se and Cs, or by studying a different element that behaves chemically in a similar manner, a 'chemical analogue', for example: studying lanthanides for actinides (De Craen et al., 2000, see Figure 4.7).

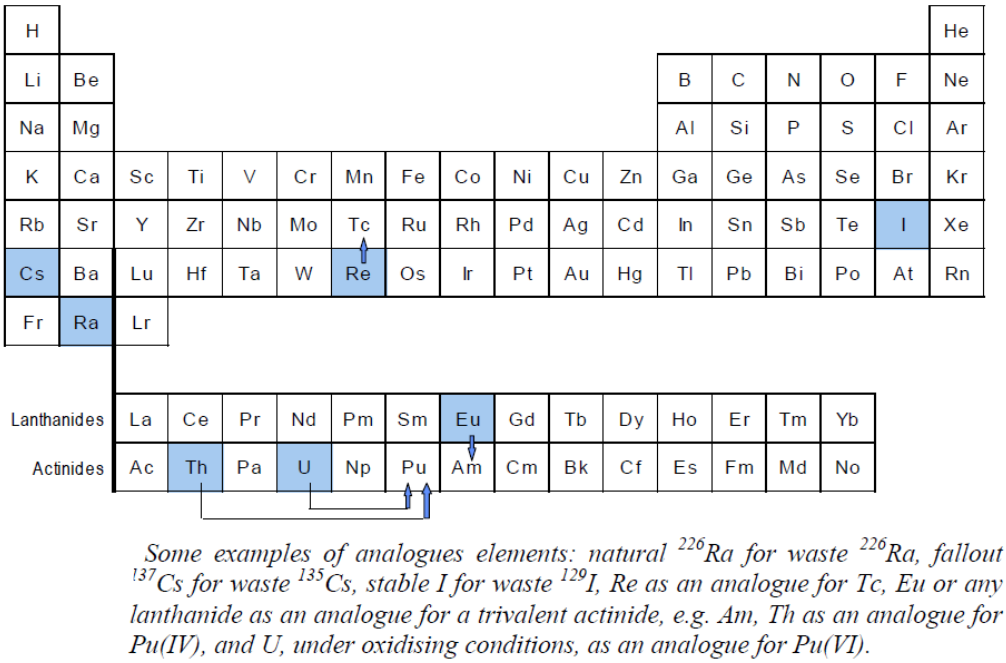

Figure 4.7: Figure from De Craen et al (2000) containing examples of analogue elements.

We can compare the values of the natural analogues in this study to those of a natural analogue study on the Boom Clay, which is a younger clay formation that is also a potential host rock for a geological disposal facility. De Craen et al. (2000) mentions a Th content between 9 and 12 ppm while the U content was generally in the range of 3 to 4 ppm. A study on the Boom Clay member in the Netherlands (Koenen and Griffioen, 2016; Koenen and Griffioen, 2013) had on average similar values for U and Th. However, the range was larger which was mainly due to the sandier layers having lower values. The latter study also had values for Cs (7 ± 3 ppm), Nd (27 ± 6 ppm), Lu (0.4 ± 0.08 ppm) and Se (1.2 ± 0.6 ppm). These values are all very similar to the average values in the samples from the Watervliet Member studied here, although our values were, on average, slightly lower which is likely due to the sandy character of this core with the relatively high quartz content acting as a diluting factor.

To explore to which mineral phases the natural analogues are associated, the correlation matrix was combined with the mineralogical results. This results in 2 main groups that explain trace element distribution relevant as natural analogue for radioactive waste disposal. The first group is the clay group containing predominantly smectite, illite, and to a lesser extent kaolinite and chlorite. This group concentrates Th, Cs, Nb, the HREE, Li and the metals

Cu, Ni, Pb, Zn. Also Se correlates well to Al in these samples. A second group contains pyrite, S, As, V, Mo and U and organic carbon. The remaining group of minerals that do not concentrate natural analogue elements consists of minerals quartz, zircon, calcite and feldspars.

Similar results were found for the Boom Clay in Belgium (De Craen et al., 2000) and the Netherlands (Koenen and Griffioen, 2016). They also found that Th, Cs and REE correlated to clay minerals. For the Boom Clay, U was correlated to pyrite and organic matter, which is similar to the samples from the Watervliet Member. In Belgium, U also correlated with apatite and calcite, which is not the case in the Watervliet samples. In the Watervliet Member samples from core KB101, calcite was only present in the top layers and the correlation with U was weak. Phosphorus content was in general very low, and apatite was also not observed in the XRD spectra. Selenium was found to be enriched in pyrite (21.6 ± 7.9 mg kg^{-1}), however these authors did not investigate the Se content in other fractions such as in clay minerals (De Cannière et al., 2010).

Trace element distributions were also studied in the Callovo-Oxfordian Clay (COX), which is a host rock for radionuclides in France (Loni et al., 2021; Montavon et al., 2022). This clay is much older (Middle/Upper Jurassic) and more indurated (lower plasticity) compared to the Boom Clay or Watervliet Clay. However, it is also of marine origin and has a comparable mineralogy, although the relative abundance differs (Jacops et al., 2017). In addition to correlations between elements derived from bulk analysis, Loni et al. (2021) and Montavon et al. (2022) have also performed sequential extractions and direct measurements on single minerals by LA-HR-ICP-MS. They found a distinct correlation between U and organic carbon, based on bulk analysis, but the analysis of individual phases showed that the U concentration in organic matter was very low. The highest U concentrations were found in apatite (32 ± 4 mg kg^{-1}), clay minerals (2.7 ± 0.8 mg kg^{-1}), and calcite (1.0 ± 0.3 mg kg^{-1}), while the content in pyrite (0.013 ± 0.004 mg kg−1) and organic matter (0.07 µg kg^{-1}) was very low. Since the clay fraction is the most abundant fraction, this corresponded to the greatest reservoir with ~65% of the U present. In our samples U was indeed also correlated to clay minerals, but also showed a clear correlation to the pyrite group.

The LA-HR-ICP-MS study on the REE Eu in COX clay concluded that also Eu is mainly present in the clay fraction (1.2 ± 0.5 µg g^{-1} of clay fraction) but was also present in the less abundant calcite (0.33 ± 0.15 µg g^{-1} of calcite). In the samples from the Watervliet Member, Eu was primarily correlated with clay minerals.

In samples from the Watervliet Member, naturally-occurring elements relevant for radioactive waste storage such as U, Se, and REE, are concentrated in clay minerals. This information can be useful in the prediction of retention of radionuclides in the long-term.

4.2 Groundwater

This section discusses the results for the groundwater samples. First, the general groundwater composition will be discussed, mainly focusing on chloride and redox parameters. Then, a number of trace elements will be discussed, which serve as a proxy for the other parameters that were measured. The concentrations for the groundwater samples are included in Appendix B.

4.2.1 General groundwater composition

Figure 4.8 shows the depth profile for chloride for the groundwater samples where concentrations above 6000 mg/l are indicative only. These highest concentrations are present in the upper 50 m of the subsurface. They were found in the deepest two filters of multi-level well B48G0100 near Ovezande and in all three filters of multi-level well B54E0238 near Sluiskil. This saline groundwater is influenced by the infiltration of seawater, which has a chloride concentration of c. 19.000 mg/l. There are also some fresh (< 150 mg Cl/l) and brackish (150 < Cl < 1000 mg/l) samples in the shallow depth range, from the first two filters of well B48G0100 and from well B54B0093 near Pyramide (IJzendijke). These are likely being influenced by infiltration of (recent) rain water; the results of the isotope analyses will likely help with the interpretation of these samples.

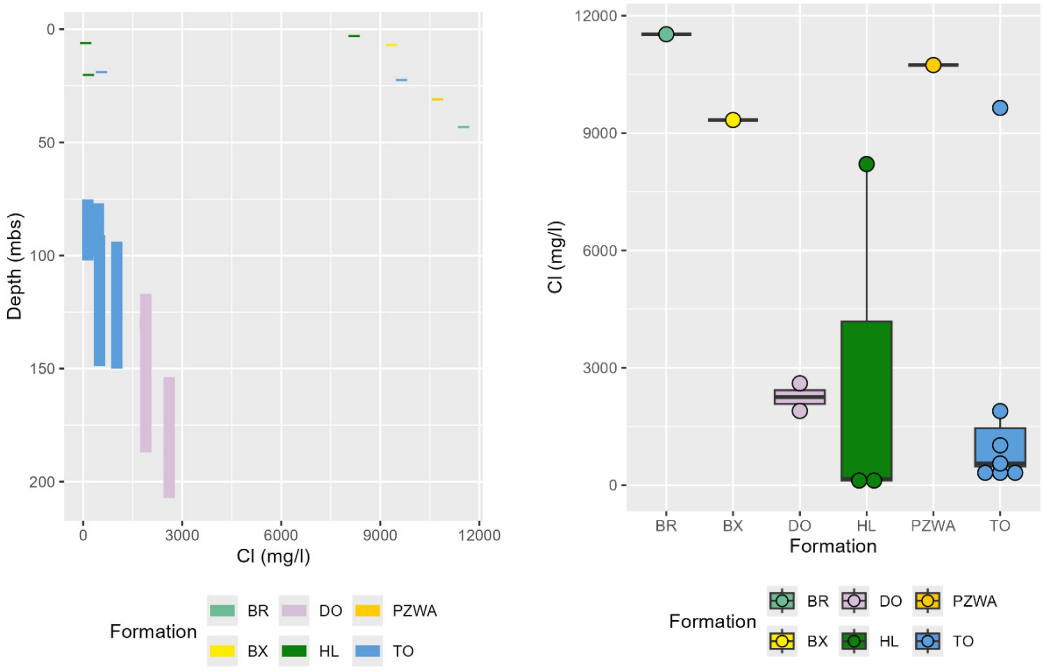

Figure 4.8: Depth plot (left side) and concentration distribution plot (right side) for chloride (values above 6000 mg/l are indicative). The colours indicate the geological formations. The bar length on the depth plot indicates the screen length for the deeper groundwater wells.

Below 50 m, there is a clear shift in chloride concentration with much lower concentrations, especially in the Tongeren Formation below the Rupel Clay (see the profiles of Figure 2.1 and Figure 3.3). Although concentrations are lower than for the shallow samples, the groundwater is still considered to be mostly brackish/saline, with chloride concentrations between 140 and 1900 mg/l for the Tongeren Formation and 1900-2600 mg/l for the samples from the Dongen Formation. The groundwater in these formations likely undergoes freshening (Figure 4.9): these samples plot above the seawater mixing line between sodium and chloride indicating that the samples are enriched in Na due to Na desorption following cation exchange under freshening conditions (Griffioen et al., 2016). Note that the two fresh groundwater samples from Holocene lie at the mixing line.

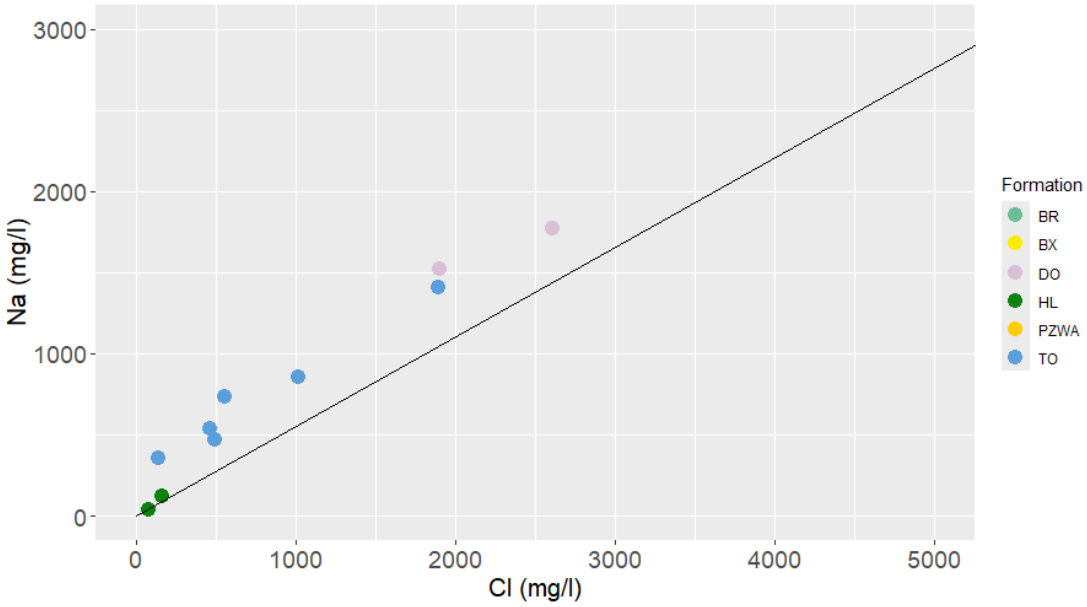

Figure 4.9: Plot of sodium versus chloride concentration for the groundwater samples, with the black line representing the mixing line between fresh rain water and seawater.

The concentrations of O_2, NO_3^-, Mn^{2+}, Fe^{2+}, SO_4^{2-}, H_2S and CH_4 in groundwater are determined by redox processes such as the decomposition of sedimentary organic material (see Figure 4.10). The redox state is a major characteristic of the groundwater composition and influences the reactive transport of microcontaminants together with pH (Griffioen et al., 2013). The redox state of the groundwater samples was determined by the classification scheme which was recently published by Broers et al. (2024) and adapted after Graf-Pannatier et al. (2000) and Pinson et al. (2020). In this classification, a distinction is made between fresh and brackish/saline water, where the sulphate to chloride ratio determines if sulphate reduction has taken place (cf. Figure 4.11).

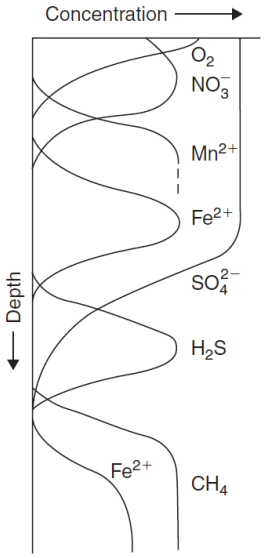

Figure 4.10: Sequence of redox-sensitive parameters with depth (Appelo & Postma, 2005)

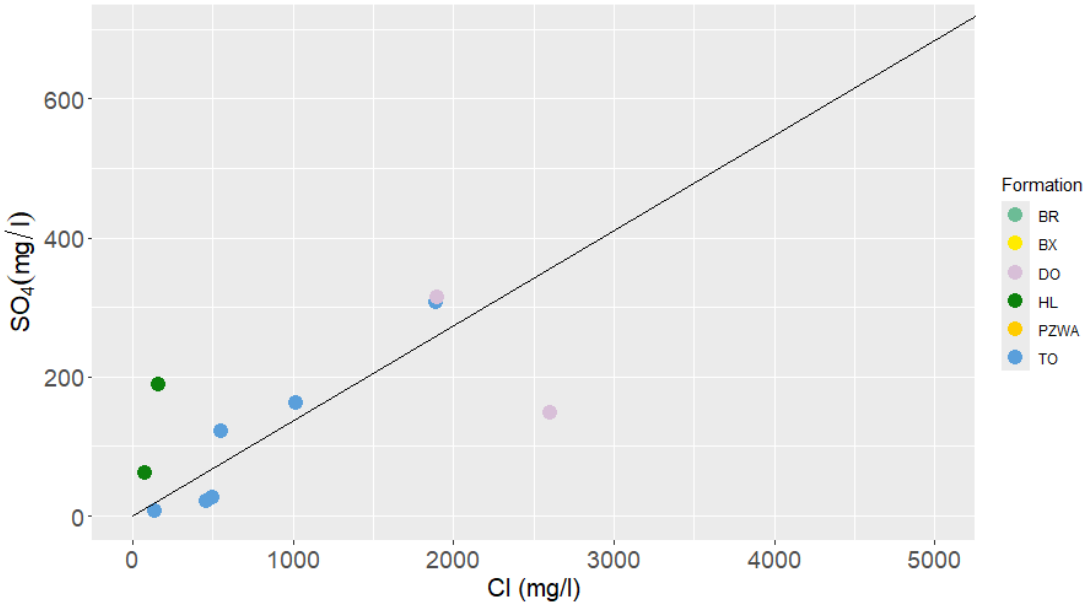

Figure 4.11: Plot of sulphate to chloride concentrations with the black line indicating the mixing line between rain water and seawater. Samples plotted below the mixing line have undergone sulphate reduction.

Most of the groundwater samples are anoxic, with the exception of the first filter of well B54E0238 at ca. 3 mbs (sample WV10), which has a dissolved oxygen concentration of 2.5 mg/l. Three samples have fresh water, the elevated sulphate (> 5 mg/l) and iron (> 0.5 mg/l) concentrations and lack of manganese (< 0.5 mg/l) place them all in the Fe-reduced redox class. The samples with elevated chloride concentration (> 200 mg/l) are classified based on the comparison between the ratio of sulfate to chloride of fresh water and the ratio of sulfate to chloride of seawater which is 0.14 (when expressed in mg/l and not mmol/l), as represented by the black line in Figure 4.11. The samples that fall below the seawater mixing line of Figure 4.11, are all SO_4-reducing. The samples above the seawater mixing line fall in the Fe-reduced redox class except the oxic one, where they all have an additional input of sulfate compared to what could be present due to dilution of seawater. Possible explanations are anthropogenic causes, especially for the shallow samples, such as historical atmospheric deposition of SO_4 from burning of coal, or an increase due to pyrite oxidation following the leaching of NO_3 from agricultural sources or exposure to air following the reclamation of tidal flats and lowering of the groundwater table due to artificial drainage (Griffioen et al., 2013).

The saturation indices (SI) with respect to several minerals and other hydrochemical characteristics were calculated using the geochemical model PHREEQC (Parkhurst & Appelo, 2013). Here, SI is 0 refers to strict thermodynamic equilibrium (practically a range of ± 0.3 can be assumed), above 0 (or +0.3) means that the solution is supersaturated and the mineral may precipitate if kinetically feasible and below 0 (or -0.3) means that the solution is undersaturated and the mineral may dissolve when present. All samples are Fe-anoxic except one that contained dissolved oxygen. The results are presented in Table 4-3. The calculated deviation from electroneutrality lies within 5% for all groundwater analyses for which it was calculated except one, where 5% deviation should be regarded as “acceptable” (Appelo and Postma, 2005).

For the other five analyses, it is not presented as the concentration for Cl as well as Na, Mg or Ca lies above the maximum concentration of the standards that were used in the ICP-OES analysis. Such results may have a systematic error and are then not very accurate.

Table 4-3. Saturation indices for some carbonate minerals, gypsum and amorphous SiO2 together with the partial CO2 pressure and electroneutrality condition for the groundwater samples.

Well+filter	Geol. Unit	Elec.Neu. error (%)	log(P_{CO2})	Calcite $CaCO_3$	Dolomite $CaMg(CO_3)_2$	Siderite $FeCO_3$	Rhodo-chrosite $MnCO_3$	Gypsum $CaSO_4{\cdot}2H_2O$	$SiO_{2(a)}$
B48G0100/1	Holocene	3.27	-1.56	0.66	0.71	1.54	0.64	-1.50	-0.07
B48G0100/4	Holocene	2.66	-2.26	1.07	2.26	1.61	0.47	-1.30	-0.51
B48G0100/5	Peize/Waalre		-1.65	0.82		1.31	0.44	-0.34	-0.83
B48G0100/6	Breda		-1.53	0.42		1.22	-0.37	-0.49	-0.76
B48G0204/1	Tongeren	-4.50	-2.94	0.55	1.45	0.72	-0.59	-3.19	-0.84
B48E0224/1	Tongeren	-4.00	-2.16	0.26	0.94	0.20	-0.50	-1.94	-0.78
B55A0340/1	Dongen	-4.71	-2.25	0.43	1.11	0.56	-0.50	-2.27	-0.43
B55A0341/1	Tongeren	-8.20	-3.01	0.55	1.38	1.06	0.80	-4.19	-1.01
B48C0196/1	Dongen	-3.35	-2.19	0.28	0.87	0.33	-0.82	-2.10	-0.41
B54E0238/1	Holocene		-0.86			oxic	0.29		-0.64
B54E0238/2	Boxtel		-0.74			1.04	0.21		-0.60
B54E0238/3	Tongeren		-0.91			1.36	-0.03		-0.48
B54B0093/1	Tongeren	1.91	-2.65	0.53	1.65	1.71	0.32	-2.63	-0.63
B48H0291/1	Tongeren	-2.01	-2.63	0.59	1.57	1.00	-0.52	-2.19	-0.91
B54F0093/1	Tongeren	-2.46	-3.04	0.42	1.12	1.07	0.42	-3.65	-0.77

The results indicate that groundwater is supersaturated for calcite, and even more supersaturated for dolomite and siderite. The aquifers thus may be calcareous where supersaturation for dolomite and siderite is commonly found in anoxic groundwater environments due to sluggish precipitation kinetics (Griffioen et al., 2013). For calcite, SI above 0.3 is rather high and less commonly found. The SI for rhodochrosite varies between -0.82 and 0.80 so availability of Mn is lacking when undersaturated. The SI values for gypsum are always below zero, implying that gypsum is not prominently present, if at all, as it is easily soluble. The values are highest for the shallow, saline samples that also contain SO_4 at high concentrations. The partial pressure of CO_2 varies more than two orders of magnitude from $10^{-3.04}$ atm to $10^{-0.74}$ atm. The low values suggest little turnover of sedimentary organic matter at the geological time scale and are mostly found in the deep wells. The high values suggest high turnover and are found in the more shallow multi-screen wells B48G0100 and B54E0238. The high values are not uncommon for shallow groundwater in the Western Netherlands where young, Holocene sediments containing degradable sedimentary organic matter are omnipresent. The SI for amorphous SiO_2 is always negative so dissolution of amorphous SiO_2 from diatomaceous algae and radiolarians is not prominent.

4.2.2 Radon

Radon was measured in the field with a Durridge RAD7 radon detector. This device can measure the ^{222}Rn (from here referred to as radon) activity in groundwater, which is a radioactive gas produced by the decay of ^{226}Ra, a member of the ^{238}U decay chain. Concentrations in groundwater are generally high due to the continuous decay of ^{226}Ra present in minerals. Radon is often used as a tracer for groundwater seepage into surface waters since activities will decline due to the short half-life of 3.8 days and degassing to the atmosphere.

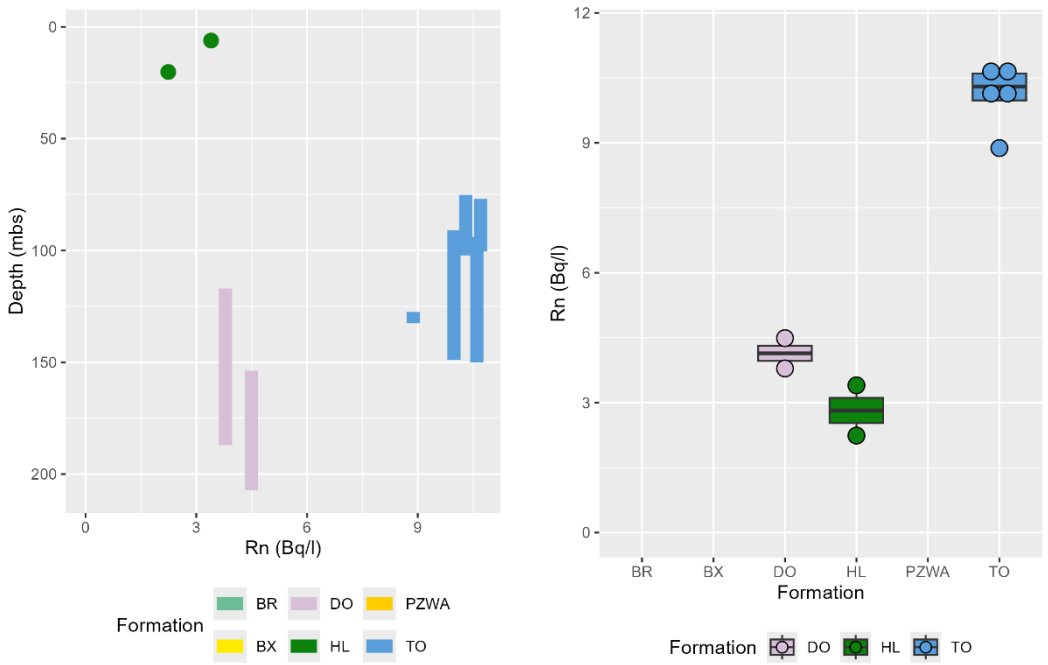

Figure 4.12: Depth plot (left side) and activity distribution plot (right side) for radon (^{222}Rn). The colours indicate the geological formations. The bar length on the depth plot indicates the filter length for the deeper groundwater wells.

Figure 4.12 shows the depth profile and activity distributions for the measured samples. Not all samples could be measured for radon, as there were some issues with excessive gas formation in samples with high EC and chloride concentrations. The results for the measured samples show the highest radon activities in the Tongeren Formation, where all samples have similar radon activity of c. 10 Bq/l. The two measured samples in the Dongen Formation and the shallow samples in the Holocene formations have lower activities relative to the samples in the Tongeren Formation. All of the measured values are within normal values found for Dutch groundwater: a measuring campaign by the RIVM in 2015 in the provinces of Overijssel en Limburg found activities between 1.6 – 16.7 Bq/l (Kwakman & Versteegh, 2015). The measured values also fall well below the parametric value of 100 Bq/l for water intended for human consumption[3].

[3] The EU Council Directive 2013/59/Euratom includes a parametric value of 100 Bq/l for ^{222}Rn. If this value is exceeded, the member states should investigate any possible health risks and take measures to restore water quality if necessary.

4.2.3 Trace elements

Given the large number of measured parameters, not all results are discussed here. The concentrations of the measured parameters are included in Appendix B. Figure 4.13 shows a correlation plot for the measured elements in groundwater, the colour indicates either a positive (blue) or negative (red) correlation, and the size of the circles and intensity of the colours indicates the strength of the correlation. Two groups can clearly be defined in the correlation plot. The first group are the rare-earth elements (REEs), which cluster at the top-left of the figure. The second group are based on the salinity of the groundwater, and cluster with chloride concentrations at the bottom right of this figure. In the next sections, four elements from the REE group are discussed as an analogue for the other element in this group (U, Th, Re, Eu), and two elements from the salinity group are discussed (Cs, Se).

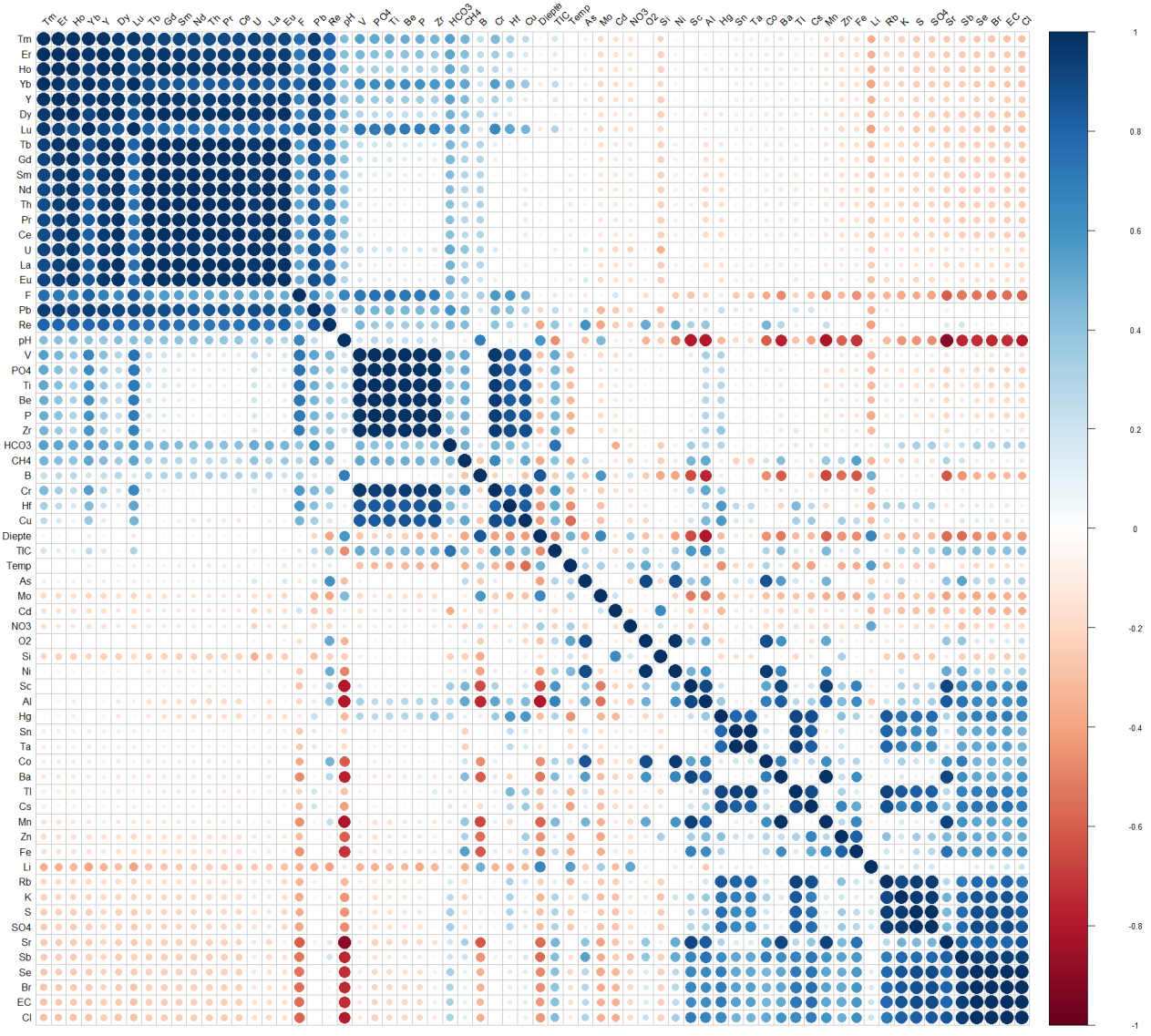

Figure 4.13: Correlation plot for the measured elements in groundwater. Only elements which were measured for all samples and above detection limits are included in this plot. The colour indicates a positive (blue) or negative (red) correlation, and the size of the dots and intensity of the colour indicates the strength of the correlation.

4.2.3.1 Uranium, thorium, rhenium and europium

Figure 4.14 and Figure 4.15 present the depth plots and concentration distributions for uranium, thorium, rhenium and europium in groundwater, used here as analogues for the REE's. Table 4-3 presents the typical seawater concentrations and, if valid, drinking water standards as reference. Uranium is present above the limit of quantification (LOQ, 0.004 µg/l) in all samples. The concentrations are on average slightly higher in the Tongeren Formation than in the other formations, but the number of samples in these formations is too low to give statistical certainty.

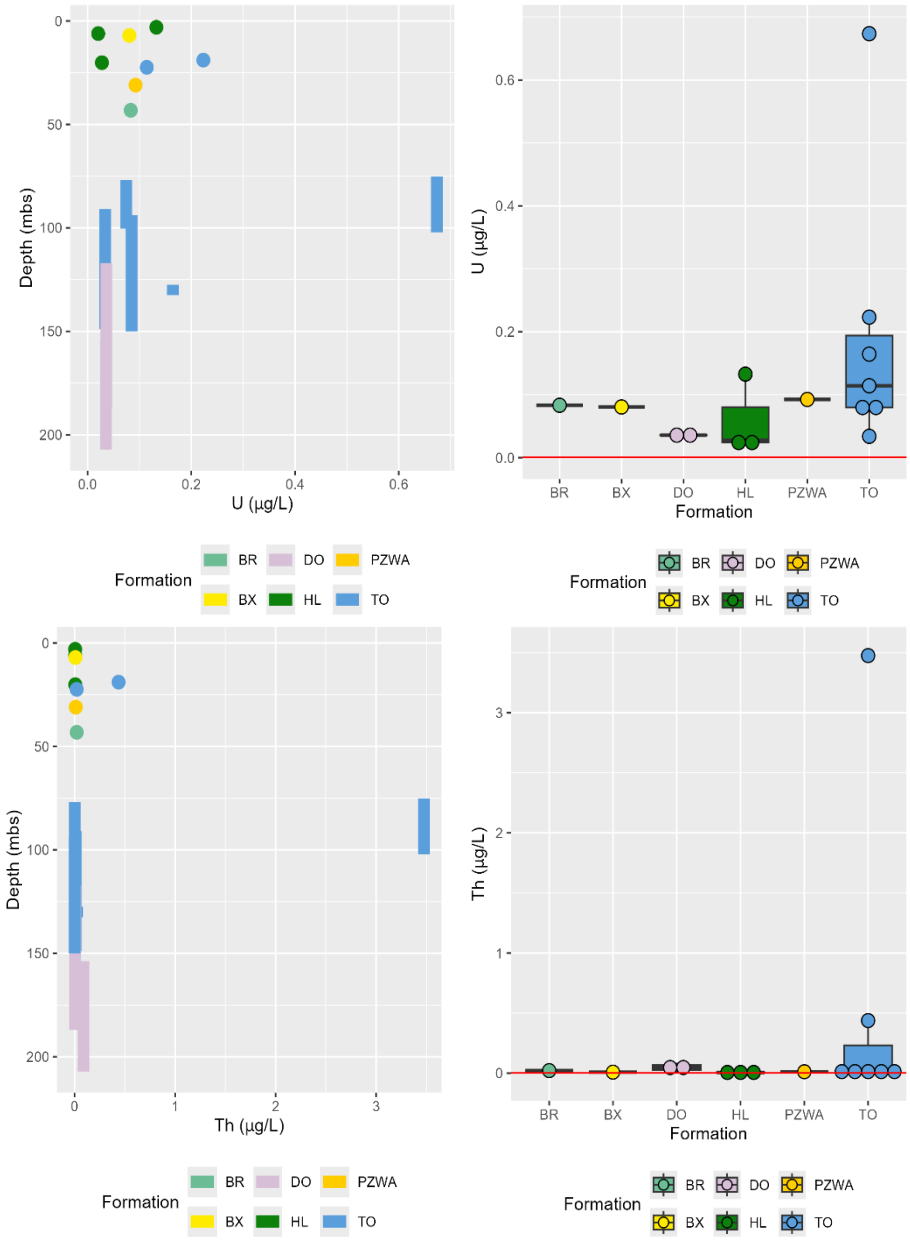

Figure 4.14: Depth plots (left side) and concentration distribution plots (right side) for uranium (top) and thorium (bottom). The colours indicate the geological formations. The bar length on the depth plot indicates the filter length for the deeper groundwater wells. The red horizontal lines on the right figures indicates the LOQ (limit of quantification).

The uranium concentrations do not seem to be correlated with depth, the concentrations for the shallow and deeper samples are fairly similar. One notable exception is the outlier in the Tongeren Formation at 90 m depth with a uranium concentration of 0.67 µg/l. This sample is from well B55A0341 in Hulst. The uranium concentrations found in this study are quite low compared to the pore water results of the Boom Clay samples reported by De Craen et al. (2000): their concentrations were reported of 4.3-11.6 µg/l for the samples from the Mol-1 borehole, and concentrations between 0.24 and 20.7 µg/l for the samples from the Doel-2b borehole. The concentrations are also considerably lower than the seawater concentration and the maximum contaminant level in drinking water of 30 µg U/l as set by the US-EPA and World Health Organisation.

Table 4-4. Seawater concentration and Dutch or international chemical standards referring to drinking water for the trace elements considered (in µg/l). The abbrevation n.e. means ''not established'' as far as known by the authors. Obtained from Hem (1985), Drinkwaterbesluit (2022), Sahoo et al. (2020), Dickson et al. (2020), Crocket et al. (2018), ATSDR (2004).

Element:	U	Th	Re	Eu	Cs	Se
Seawater	3	0.05	0.008	0.144 to 0.343	0.5	4
Drinking water limit	30 (USA+WHO)	n.e.	n.e.	1050#	n.e.	20 (Dutch)

indicative admissible drinking water concentration calculated by De Boer et al. (1996).

The results for thorium are similar to uranium. In general, the concentrations are low but most samples measure above the LOQ of 0.001 µg/l, with the exception of sample WV14 (B48H0291) which is below the LOQ. Again there does not seem to be a relation with depth; the concentrations for all formations are in a similar range. The outlier of well B55A0341 is again present at 3.5 µg/l. This is within the range that was found for the pore-water samples for the Boom Clay and surrounding layers of borehole Mol-1 (0.027-12.2 µg/l), but slightly higher than the concentrations for the Doel-2b borehole which were mainly below the detection limit (< 0.25 µg/l). Most of our samples are also below that boundary where two of them lie between this value and the typical seawater concentration and 12 samples lie below the seawater concentration. There are 7 naturally occurring isotopes of thorium but none of them is stable. There is therefore no international chemical drinking water limit that can be used as a reference but there are standards for radioactivity of drinking water in addition to the specific one for radioactive radon. So, the presence of thorium is taken into account in that way.

Figure 4.14 show the results for rhenium and europium. The concentrations for rhenium are all very low, below 0.01 µg/l. The shallow samples are generally higher in concentration than the deeper samples. The majority of the deeper samples are below the LOQ of 0.0005 µg/l. The highest concentration of 0.0071 µg/l is again found in well B55A0341. It is less of an outlier than it is for the other parameters and lies just below the seawater concentration. Rhenium is one of the rarest elements in the continental crust which may be a reason why no drinking water limits have been established.

Europium shows again a very similar pattern to the other parameters. Here, concentrations are slightly higher for the shallow samples than for the deeper samples, where all measured screens are above the LOQ of 0.0002 µg/l. The outlier of well B55A0341 is again present with a concentration of 0.3079 µg/l, which lies within the range of seawater concentrations. The other concentrations were 2.5 or more times lower than the lower limit for the seawater concentration.

These results are again in line with what was found for the pore samples for the Boom Clay of De Craen et al. (2000). Their concentrations were mostly below the detection limit of 0.2 µg/l with two samples above this limit at 0.22 and 0.44 µg/l. Janssen & Verweij (2003) studied Eu and 6 other REEs at the drinking water production site Vierlingsbeek at the Peel Horst. They found that the Eu concentration in deep groundwater (c. 20-35 m below surface) was commonly below detection limit of 0.046 µg/l. More shallow groundwater had Eu concentrations up to 4.56 µg/l. Deep samples (22 – 28 m) at one well also had elevated concentrations up to 5.19 µg/l. The elevated concentrations in shallow groundwater coincided with high NO_3 and DOC concentrations: up to 270 mg/l and 1.71 mg/l. Deeper groundwater contained dissolved Fe (up to 22.00 mg/l) and commonly low DOC (0.15 mg/l or less). It was concluded that the studied REEs probably had a natural origin despite the mutual occurrence with high NO_3 concentrations due to manure spreading. The low Eu concentrations in Fe-anoxic groundwater show similarity with the observations for anoxic groundwater in Zeeland. It is believed that europium is not particularly toxic especially when compared to other heavy metals (Rim et al., 2013). Upon result, no international drinking water limit was found for purpose of referencing.

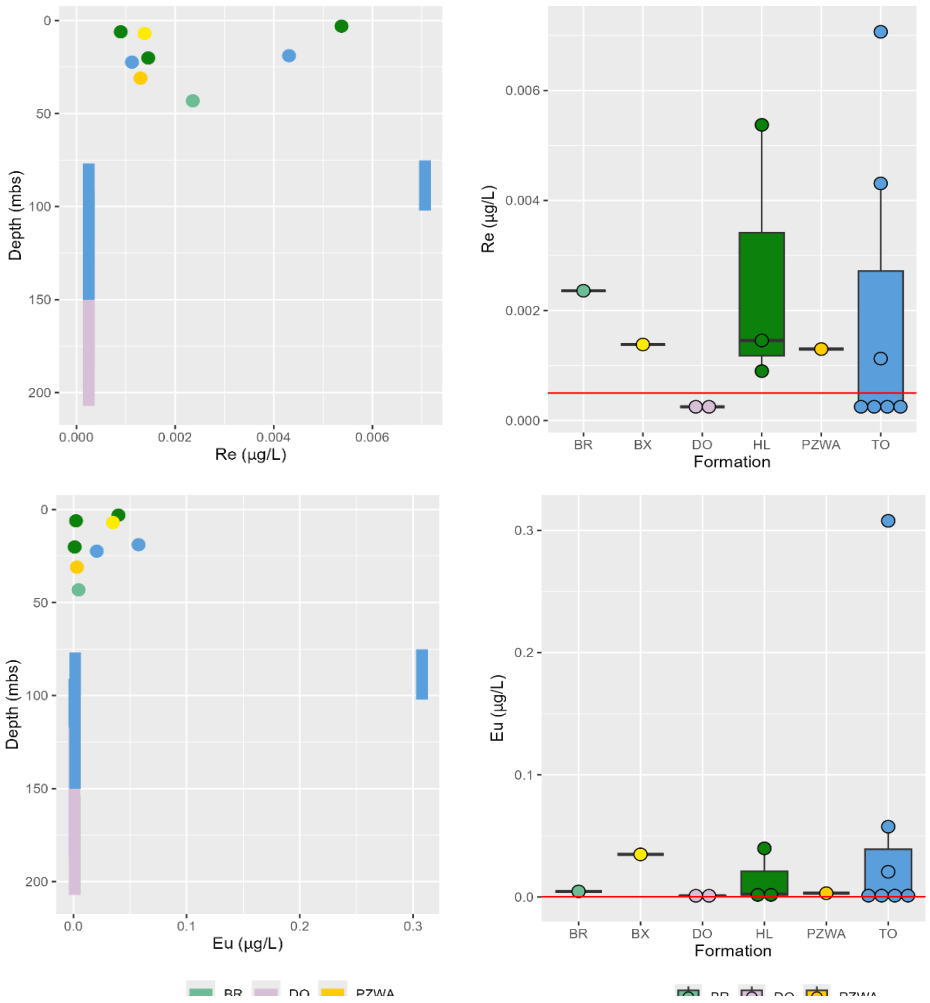

Figure 4.15: Depth plots (left side) and concentration distribution plots (right side) for rhenium (top) and europium (bottom). The colours indicate the geological formations. The bar length on the depth plot indicates the filter length for the deeper groundwater wells. The red horizontal lines on the right figures indicates the LOQ (limit of quantification).

4.2.3.2 Caesium and Selenium

Figure 4.16 shows the concentration patterns for caesium and selenium. As the correlation plot of Figure 4.13 shows, the concentrations of these two parameters closely follow the salinity patterns of the groundwater samples. The concentrations for Cs are low (below 0.3 µg/l but all samples except one are above the LOQ of 0.003 µg/l). The highest concentration is found for well B48G0100 in the Breda Formation, which is also the sample with the highest indicative chloride concentration. The well which produced the outliers for the parameters mentioned in the paragraphs above (B55A0341) does not show significantly higher Cs concentrations than the other samples in the deeper parts of the Tongeren Formation. All concentrations fall below the seawater concentration of 0.5 µg/l. The results from the Boom Clay pore water samples in the Doel-2b borehole show Cs concentrations between < 0.1 to 1.82 µg/l. The groundwater samples are all within this range. No comparison with a chemical drinking water standards can be made. Here, it is the general opinion that it is unlikely that stable caesium affects the health of people; ATSDR, 2004).

The concentrations for Se are much higher than the other mentioned parameters with a maximum of 132 µg/l. Ten samples also have concentrations above the seawater concentration of 4 µg/l. This is opposite to the general findings for the other five trace elements considered and brings forward that the subsurface is likely an overall source and not a sink. The five highest concentrations are found in shallow, saline groundwater. These concentrations are also above the Dutch drinking water standard of 20 µg Se/l (Table 4-3) whereas the others are below. The concentrations in the deeper aquifers of the Tongeren Formation and the Dongen Formation are lower: they range from 0.862 to 16.9 µg/l.

4.2.3.3 Geochemical controls on the natural analogues

Groundwater in the deep, buried aquifers likely has a large travel time of thousands of years or even more and no anthropogenic contamination has to be expected accordingly. For the shallow aquifers, considerable ages of hundreds to thousands of years may also be expected for groundwater sampled at tens of meters depth. This may also imply that no anthropogenic contamination happened during infiltration. Subsurface immobilisation of U, Th, Re, Eu and Cs from infiltrated, diluted seawater may have happened for the brackish and saline samples. The subsurface may also be a source by e.g. weathering especially for the fresh samples but the concentrations stay low. Selenium is an exception for which mobilisation to concentrations above the seawater concentration frequently happened. The role of geochemical processes has not been explored any further and is complex for the redox-sensitive elements U, Se and Re, somewhat more straightforward for tetravalent Th and predominantly trivalent Eu, and rather straightforward for monovalent Cs and Rn as noble gas. Here, one main difference is that Cs forms well soluble salts and the first five elements do also form insoluble salts.

The sediment data allow assumptions on the geo-availability of the elements of interest. A strong association with clay minerals as observed for e.g. Th, Cs, and the heavy REE may suggest that their natural geo-availability is low where such elements are incorporated in the crystal structure. Data on the composition of pore water in the Watervliet Member is not yet available. This enables a comparison between the Watervliet Member as a confining layer and the surrounding sand layers as aquifer. From this, one can assess whether the Watervliet Member acts as a source or sink for the elements of interest compared to the aquifers.

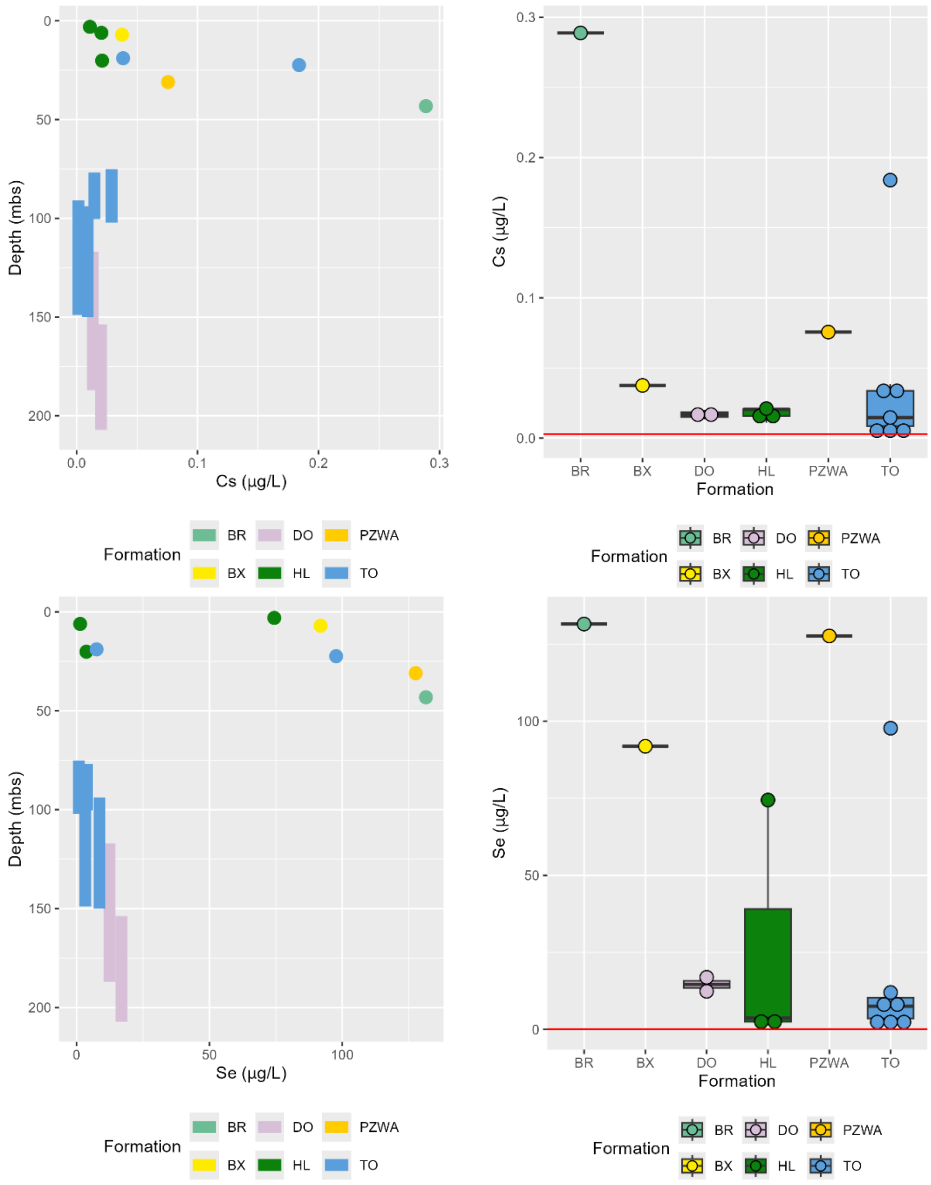

Figure 4.16: Depth plots (left side) and concentration distribution plots (right side) for caesium (top) and selenium (bottom). The colours indicate the geological formations. The bar length on the depth plot indicates the filter length for the deeper groundwater wells. The red horizontal lines on the right figures indicates the LOQ (limit of quantification).

5 Conclusions

An environmental geochemical study is presented on the composition of the Paleogene Watervliet Member in Zeeland and groundwater in the surrounding Paleogene and younger sandy units within the framework of potential disposal of radioactive waste in argillaceous sediments.

The Watervliet Member was studied in cores from borehole KB101 drilled in Borsele (Zeeland). Even though the originally anoxic sediment in the cores was partially oxidized due to non-ideal storage conditions, an adequate geochemical characterization could be carried out. The 25 m thick trajectory of the Watervliet Member consisted of an alternation of more clayey and sandy layers. Overall, half of the samples was classified as clay while the others classify as sand or silt. The top contained high carbonate content, while this was absent in the lower 15 m. The main minerals were quartz, clay minerals, feldspars and calcite. Also glauconite was abundant. To better understand radionuclide behaviour in the context of radioactive waste disposal, the naturally-occurring elements/radionuclides with analogue geochemical behaviour to these radionuclides were studied. In this study, U, Th, Cs, Se and rare earth elements (REE) were analyzed for both their content and the mineral phase to which they are associated. The U content is on average 2 ± 0.9 ppm, Th 7 ± 2 ppm, Se 1 ± 0.3 ppm, Cs 5 ± 2 ppm, Lu 0.22 ± 0.05 ppm and Re 7 ± 3 ppb. All of these elements were correlated to clay minerals. Uranium and selenium were also correlated to pyrite. These values are slightly lower than those in other clay formations such as the Boom Clay in Belgium and the Netherlands. The difference can be explained by the lower clay content, and in general sandier character of the Watervliet Member at borehole KB101. This property of the Watervliet Member is a topic of attention with respect to the barrier function of this geological unit or its clay layers as the Watervliet Member is lithologically characterised as a unit of alternating sand and clay layers.

Groundwater composition was studied from 15 wells in Paleogene and younger aquifer as present in central and Southern Zeeland. Two groups are recognised compositionally: first, deep buried Paleogene aquifers containing fresh to saline groundwater from probably Pleistocene age and infiltrated in Belgium or near the national border. Second, shallow aquifers with either fresh or very saline groundwater from likely Holocene age. All groundwater was found to be pH neutral, saturated for calcite and mostly anoxic. The observed values for the radioactivity of Rn is typical for Dutch groundwater and was highest for groundwater samples from the buried, Paleogene Tongeren Formation. Six more trace elements were studied in more detail. Selenium concentrations were highest with maximum of 130 µg/l and frequent exceedances of the seawater concentration. The U, Th, Re, Eu and Cs concentrations were 1. always below 0.5 µg/l (except one outlier for Th), 2. below the respective seawater concentrations except some exceptions and 3. predominantly above the respective limits of quantification. The concentrations were higher in the shallow aquifers than in the deeper, buried aquifers except one deep well with outliers for U, Th and Eu. A comparison with - indicative or legally established - drinking water standards can be made for U, Se and Eu. For the brackish and saline groundwater, immobilisation of U, Th, Re, Eu and Cs from (diluted) sea water may have happened whereas geochemical mobilisation happened for Se. Radon gets actively produced in the subsurface. The U and Eu concentrations lie below these standards and 5 shallow, saline samples show exceedances for Se while the rest lies below.

This research project has resulted in a baseline study of the environmental geochemical and mineralogical composition of the Paleogene Watervliet Member and trace elements composition of Paleogene and younger groundwater in central and southern Zeeland. The results are of general use and specifically for risk assessment of the fate of radionuclides in comparable groundwater environments.

6 References

Klik of tik om tekst in te voeren.
Appelo, C.A.J., Postma, D. (2005). Geochemistry, groundwater and pollution, 2nd edition. A.A. Balkema Publishers, Leiden.

ATSDR (2004). Public health statement Cesium CAS#: 7440-46-2. Agency for Toxic Substances and Disease Registry. Department of health and human services, public health service.

Beekman, H.E., Eggenkamp, H.G.M. & Appelo, C.A.J. (2011). An integrated modelling approach to reconstruct complex solute transport mechanisms - Cl and δ37Cl in pore water of sediments from a former brackish lagoon in The Netherlands. Applied Geochemistry (26), 257–268.

Blaser, P.C., Coetsiers, M., Aeschbach-Hertig, W., Kipfer, R., Van Camp, M., Loosli, H.H. & Walraevens, K. (2010). A new groundwater radiocarbon correction approach accounting for palaeoclimate conditions during recharge and hydrochemical evolution: The Ledo-Paniselian Aquifer, Belgium. Applied Geochemistry (25), 437-455.

Broers, H.P., Kivits, T, Sültenfuß, J. ten Harkel, M., van Vliet, M. (2024). Mobility and persistence of pesticides and emerging contaminants in age-dated and redox-classified groundwater under a range of land use types. Science of the Total Environment 954, 176344

Coetsiers, M., Blaser, P., Martens, K. & Walraevens, K. (2009). Natural background levels and threshold values for groundwater in fluvial Pleistocene and Tertiary marine aquifers in Flanders, Belgium. Environ. Geol. (57), 1155–1168.

Crocket KC, Hill E, Abell RE, Johnson C, Gary SF, Brand T and Hathorne EC (2018). Rare Earth Element Distribution in the NE Atlantic: Evidence for Benthic Sources, Longevity of the Seawater Signal, and Biogeochemical Cycling. Front. Mar. Sci. 5:147.

De Cannière, P., Maes, A., Williams, S., Bruggeman, C., Beauwens, T., Maes, N., & Cowper, M. (2010). Behaviour of selenium in Boom Clay. *External Report, SCK• CEN-ER-120*.

De Craen, M., Delleuze, D., Volckaert, G., Sneyers, A., & Put, M. (2000). The Boom Clay as natural analogue. R-3444. Waste & Disposal Department, SCK•CEN, Mol, Belgium.

Dickson, A.J., Yu-Te Hsieh, Allison Bryan (2020). The rhenium isotope composition of Atlantic Ocean seawater. Geochimica et Cosmochimica Acta (287), 221–228.

Dooley, G.H. (2001). Baseline Concentrations of Arsenic, Beryllium and Associated Elements in Glauconite and Glauconitic Soils in the New Jersey Coastal Plain. Report by the New Jersey Department of Environmental Protection Division of Science, Research and Technology Geological Survey.

Drinkwaterbesluit (2022). Besluit van 8 november 2022 tot wijziging van het Drinkwaterbesluit, het Besluit kwaliteit leefomgeving en enkele andere algemene maatregelen van bestuur in verband met de omzetting van EU-Drinkwaterrichtlijn 2020/2184 (herschikking). Staatsblad 2022 450

Gleyzes, C., Tellier, S., & Astruc, M. (2002). Fractionation studies of trace elements in contaminated soils and sediments: a review of sequential extraction procedures. *TrAC Trends in Analytical Chemistry*, *21*(6-7), 451-467.

Graf-Pannatier, E., Broers, H.P., Venema, P. & van Beusekom, G. (2000). A new process-based hydro-geochemical classification of groundwater. Application to the Netherlands National Monitoring System. TNO-report NITG 00-143-B, Netherlands Institute of Applied Geoscience TNO – National Geological Survey.

Griffioen, J., Verweij, H. & Stuurman, R. (2016). The composition of groundwater in Palaeogene and older formations in the Netherland. A synthesis. Netherlands Journal of Geosciences 95(3), 349-372.

Griffioen, J., Vermooten, S. & Janssen, G. (2013). Geochemical and paleohydrological controls on the composisiton of shallow groundwater in the Netherlands. Applied Geochemistry 39, 129-149

Hem, J.D. (1985). Study and interpretation of the chemical characteristics of natural water. U.S. Geol. Survey Water-Supply Paper 2254, 3rd ed.

Huerta-Diaz, M. A., & Morse, J. W. (1992). Pyritization of trace metals in anoxic marine sediments. *Geochimica et Cosmochimica Acta*, *56*(7), 2681-2702.

Hutchison, A., Hartley, A., Hole, M., Whear, E., & Preston, J. (2001). High resolution geochemical and petrographical correlation of deep marine Palaeocene sandstones from the Foinaven Field, West of Shetland. *Petroleum Geoscience*, *7*(2), 123-129.

Janssen, R.P.T. & Verweij, W. (2003). Geochemistry of some rare earth elements in groundwater, Vierlingsbeek, The Netherlands. Water Research (37), 1320-1350.
Kwakman, P.J.M.& Versteegh, J.F.M. (2016). Radon-222 in ground water and finished drinking water in the Dutch provinces Overijssel and Limburg. Measuring campaign 2015. RIVM Letter report 2016-0048, National Institute for Public Health and the Environment.

Koenen, M., & Griffioen, J. (2016). Characterisation of the geochemical heterogeneity of the Rupel Clay Member in the Netherlands. *Netherlands Journal of Geosciences*, *95*(3), 269-281.

Koenen, M., & Griffioen, J. (2013). *Mineralogical and geochemical characterization of the Boom Clay in the Netherlands*. Report OPERA-PU-TNO521-1: 107 pp.

Loni, Y.H., David, K., Ribet, S., Lach, P., Lerouge, C., Madé, B., Bailly, C., Grambow, B. and Montavon, G., (2021). Investigation of europium retention on Callovo-Oxfordian clay rock (France) by laser ablation inductively coupled plasma mass spectrometry (LA-ICP-MS) and percolation experiments in microcells. *Applied Clay Science*, *214*, p.106280.

Montavon, G., Solange Ribet, Y. Hassan Loni, F. Maia, C. Bailly, Karine David, Catherine Lerouge, B. Madé, J. C. Robinet, and Bernd Grambow. (2022). Uranium retention in a Callovo-

Oxfordian clay rock formation: From laboratory-based models to in natura conditions. *Chemosphere*, *299*, 134307.

Parkhurst, D.L. & Appelo, C.A.J. (2013). Description of Input and Examples for PHREEQC Version 3—A Computer Program for Speciation, Batch-Reaction, One-Dimensional Transport, and Inverse Geochemical Calculations. US Geological Survey Techniques and Methods, Book 6, Chapter A43, 497 p.

PCR (2013). Preliminary ground investigations report - project KCB2 Borssele, the Netherlands. Redacted version prepared for COVRA, www.covra.nl.

Pinson , S., Malcuit, E., Gourcy, L., Ascott, M., Broers, H.P., van Vliet, M., Hinsby, K., Thorling, L., Rosenbom, A. & Christophi, C. (2020). Assessment of attenuation patterns for a number of relevant European settings. GeoERA HOVER WP5, deliverable 5.4.

Raiswell, R., & Plant, J. (1980). The incorporation of trace elements into pyrite during diagenesis of black shales, Yorkshire, England. *Economic Geology*, *75*(5), 684-699.

Rim, K.T., Koo, K.H. & Park, J.S. (2013). Toxicological Evaluations of Rare Earths and Their Health Impacts to Workers: A Literature Review. Saf Health Work (4), 12-26.

Sahoo, V.N. Jha , A.C. Patra, S.K. Jha, M.S. Kulkarni (2020). Scientific background and methodology adopted on derivation of regulatory limit for uranium in drinking water – A global perspective. Env. Adv. (2), 100020.

Schout G, Griffioen J, Hartog N, Eggenkamp HGM, and Cirkel DG. (2024). Methane occurrence and origin in Dutch groundwater: from shallow aquifers to deep reservoirs. Netherlands Journal of Geosciences, Volume 103, e24.

Vandenberghe, N., Hilgen F.J. & Spijer, R.P. (2012). Chapter 28 - The Paleogene Period. In ‘’The Geologic Time Scale”, Elsevier, p. 855-921.

Vermoortel, Y., Mahauden, M. & De Breuck, W. (1996). Grondwateronderzoek Diepe Zandlagen, Fase II. Laboratorium voor Toegepaste Geologie en Hydrogeologie, Geologisch Instituut, Universiteit Gent.

Zaadnoordijk et al. (2022). Hydrogeologisch basismodel Zuid-Nederland. TNO rapportno. TNO 2022 R11720.

Zeelmaekers, E. (2011). Computerized qualitative and quantitative clay mineralogy: introduction and application to known geological cases. PhD Thesis. Katholieke Universiteit Leuven. Groep Wetenschap en Technologie: Heverlee. ISBN 978-90-8649-414-9. XII, 397 pp.

7 Undersigning

Name and undersigning 2e reader

ValidSigned by Joris Dijkstra
on 2024-12-19 10:51:58

Dr.ir. J.J. Dijkstra

Undersigning

ValidSigned by Jasper Griffioen
on 2024-12-18 13:02:41

Prof.Dr. J. Griffioen
Author

Authorization release

ValidSigned by Yvonne Schavemaker
on 2024-12-18 12:50:37

Y.A. Schavemaker MSc
Research Manager

Appendix A

Results Sediment

A.1 XRF – Fusion bead

Oxide/Element	Al2O3	CaO	Fe2O3	K2O	MgO	MnO	Na2O	P2O5	SiO2	TiO2	Ba	Cr	Ni	Sr	Zr
Sample code	%	%	%	%	%	%	%	%	%	%	ppm	ppm	ppm	ppm	ppm
101-95	6.58	0.29	2.70	2.88	0.63	0.01	1.04	0.03	81.89	0.45	488	93	16	92	406
101-96	12.15	0.21	6.19	3.07	1.74	0.02	1.04	0.04	67.94	0.78	378	138	50	64	279
101-97	6.63	6.08	5.11	2.73	1.05	0.02	0.76	0.11	69.58	0.48	326	119	15	267	539
101-98	7.47	15.77	4.06	2.13	1.11	0.03	0.74	0.10	52.90	0.47	268	98	20	656	353
101-99	7.23	3.32	5.64	2.85	1.17	0.01	0.78	0.08	72.89	0.46	344	120	19	184	381
101-100	12.35	12.91	4.72	2.55	1.99	0.03	0.77	0.06	48.00	0.63	269	100	25	513	207
101-101	10.48	16.79	3.90	2.25	1.70	0.03	0.69	0.07	45.36	0.55	239	97	18	617	186
101-102	11.22	10.02	4.69	2.64	1.79	0.02	0.70	0.07	55.98	0.61	293	108	26	443	279
101-103	7.61	3.94	5.04	2.86	1.26	0.02	0.71	0.08	71.76	0.56	390	140	16	221	514
101-104	11.86	0.68	5.48	3.00	1.65	0.02	0.78	0.07	69.21	0.77	429	142	27	138	385
101-105	9.99	0.47	5.58	2.84	1.24	0.02	0.82	0.05	70.97	0.67	430	119	26	142	305
101-106	7.49	0.51	6.68	3.47	1.35	0.01	0.64	0.06	74.55	0.47	379	166	18	103	426
101-107	9.46	0.61	7.05	3.43	1.64	0.01	0.52	0.06	71.61	0.51	353	155	21	108	287
101-107d	10.13	0.54	7.16	3.53	1.75	0.01	0.55	0.06	70.65	0.55	357	158	23	105	282
101-108	7.03	0.35	6.77	3.47	1.36	0.01	0.47	0.06	75.54	0.37	337	148	18	85	354
101-109	7.01	0.54	6.67	3.55	1.33	0.01	0.51	0.07	75.28	0.37	350	148	19	108	346
101-110	11.17	0.43	6.39	3.37	1.75	0.01	0.53	0.06	68.34	0.58	355	144	25	101	314
101-111	9.27	0.54	7.06	3.48	1.44	0.01	0.49	0.08	69.87	0.47	347	133	22	116	326
101-112	17.51	0.21	6.56	3.52	2.34	0.01	0.49	0.05	58.34	0.82	339	152	36	97	185
101-113	16.09	0.15	7.06	3.30	2.10	0.01	0.50	0.04	59.49	0.86	344	149	38	76	215
101-114	6.29	0.31	5.19	3.30	0.97	0.01	0.51	0.05	78.89	0.33	380	-	-	83	415
101-115	9.88	0.20	5.69	3.17	1.34	0.01	0.54	0.04	72.39	0.53	371	140	24	68	307
101-116	5.48	0.23	5.41	2.93	0.88	0.01	0.42	0.04	79.69	0.28	334	121	15	64	271
101-117	9.91	0.35	6.57	3.40	1.40	0.01	0.52	0.05	69.33	0.50	349	134	24	86	218
101-118	12.85	0.36	5.85	3.47	1.65	0.01	0.60	0.05	67.28	0.70	384	146	31	92	253

A.2 XRF pressed pellet

Oxide/Element	Al2O3	CaO	Fe2O3	K2O	MgO	MnO	Na2O	P2O5	SiO2	TiO2	As	Ba	Ce	Cr	Cu
Sample code	%	%	%	%	%	%	%	%	%	%	ppm	ppm	ppm	ppm	ppm
101-95	7.03	0.21	2.75	2.78	0.74	0.01	1.33	0.04	77.49	0.50	4	472	47	79	0
101-96	11.15	0.13	5.37	2.73	1.68	0.02	1.27	0.05	65.77	0.76	8	352	57	116	13
101-97	7.12	6.38	5.17	2.53	1.25	0.01	0.81	0.11	64.77	0.53	3	251	47	103	14
101-98	7.27	14.64	4.37	2.12	1.30	0.02	0.70	0.09	53.14	0.47	6	154	43	80	24
101-99	7.31	3.58	5.53	2.65	1.28	0.01	0.80	0.07	68.16	0.50	4	288	46	105	11
101-100	11.61	12.94	4.79	2.35	2.04	0.02	0.70	0.06	49.94	0.64	7	168	47	84	13
101-101	11.50	16.46	4.63	2.22	2.09	0.03	0.64	0.05	45.94	0.60	7	125	42	76	16
101-102	11.37	8.97	5.09	2.56	1.95	0.01	0.67	0.07	56.09	0.66	5	227	45	94	8
101-103	7.88	3.73	5.21	2.78	1.44	0.01	0.72	0.08	67.57	0.57	4	301	53	121	20
101-104	11.75	0.62	5.18	2.73	1.71	0.01	0.81	0.06	64.14	0.79	7	389	54	112	10
101-105	9.56	0.47	5.92	2.62	1.29	0.01	0.88	0.06	64.75	0.67	6	405	47	95	17
101-106	7.67	0.46	6.78	3.37	1.53	0.01	0.67	0.07	68.13	0.51	4	357	55	146	6
101-107	8.64	0.55	6.67	3.20	1.60	0.01	0.54	0.06	68.14	0.48	5	301	56	125	8
101-107d	8.68	0.44	6.66	3.21	1.61	0.01	0.54	0.06	68.32	0.49	5	316	55	127	7
101-108	7.12	0.33	6.76	3.37	1.47	0.01	0.52	0.06	69.69	0.40	5	322	54	132	3
101-109	7.18	0.52	6.50	3.35	1.43	0.01	0.55	0.07	70.38	0.41	5	322	56	132	10
101-110	11.26	0.27	5.92	3.10	1.78	0.01	0.56	0.05	63.92	0.62	8	315	58	126	20
101-111	9.53	0.37	6.51	3.18	1.58	0.01	0.55	0.07	65.13	0.52	7	315	56	122	7
101-112	13.86	0.46	6.67	3.15	1.95	0.01	0.55	0.05	58.81	0.70	15	298	64	127	12
101-113	15.11	0.20	6.22	2.91	1.96	0.01	0.56	0.04	57.64	0.85	17	301	72	145	176
101-114	6.51	0.23	5.23	3.16	1.07	0.01	0.56	0.05	73.67	0.36	5	353	51	110	8
101-115	10.02	0.24	5.99	3.10	1.43	0.01	0.56	0.05	66.95	0.55	9	339	62	112	15
101-116	6.26	0.20	5.27	2.86	1.03	0.01	0.48	0.05	74.74	0.34	6	301	53	104	3
101-117	9.29	0.29	5.78	3.11	1.36	0.01	0.56	0.04	67.61	0.50	7	322	54	115	8
101-118	13.80	0.13	5.78	3.11	1.72	0.01	0.66	0.03	61.89	0.77	10	352	63	136	40

	Ga	Hf	La	Nb	Nd	Ni	Pb	Pr	Rb	S	Sc	Sn	Sr	Th	U	V	Y	Zn	Zr	Rh
Sample code	ppm	ppm	ppm	ppm	ppm	ppm	ppm	ppm	ppm	ppm	ppm	ppm	ppm	ppm	ppm	ppm	ppm	ppm	ppm	kcps
101-95	5	11	23	8	23	15	10	6	74	2384	8	3	102	8	1	61	16	53	478	36
101-96	11	8	28	11	27	46	10	7	107	6248	16	5	75	12	3	110	25	114	332	33
101-97	6	14	27	8	26	20	10	7	80	5859	11	1	287	12	1	77	19	49	556	30
101-98	7	11	27	7	25	23	10	7	73	3554	13	0	638	11	3	79	19	66	343	28
101-99	7	10	24	8	24	22	8	6	84	5584	13	2	204	9	2	71	16	45	408	31
101-100	12	7	25	11	23	32	12	6	106	3443	17	3	501	11	0	121	17	73	234	29
101-101	13	5	32	10	28	31	13	7	100	2392	17	5	628	6	1	124	17	73	173	28
101-102	13	8	27	11	25	31	12	6	106	1960	16	0	406	14	1	113	17	71	279	30
101-103	7	11	20	9	21	19	11	6	92	2003	16	1	221	4	1	97	18	53	490	31
101-104	13	11	27	13	26	31	15	7	110	6800	16	0	136	8	2	108	20	73	447	33
101-105	11	8	26	10	24	29	14	6	91	13846	11	3	159	8	2	82	16	53	355	32
101-106	8	9	28	8	27	17	10	7	112	5884	14	2	127	3	2	111	17	47	420	31
101-107	9	7	30	9	28	16	10	8	120	5851	12	2	113	10	2	114	16	50	314	31
101-107d	9	8	28	9	27	17	10	7	120	5312	13	3	109	11	3	114	17	49	331	31
101-108	8	7	25	7	25	16	9	7	114	6003	12	0	102	6	3	107	15	42	356	31
101-109	6	9	29	7	28	18	10	7	113	6506	11	3	128	1	3	109	16	44	396	31
101-110	13	7	34	11	31	27	12	8	133	7165	12	5	100	7	3	130	21	69	330	33
101-111	10	7	28	9	27	22	13	7	120	9471	15	2	114	7	3	116	18	56	357	31
101-112	15	7	33	13	31	32	21	8	153	9659	16	5	133	6	3	160	21	78	271	31
101-113	18	5	41	16	39	45	21	10	156	11405	20	1	101	10	4	173	26	158	242	32
101-114	7	9	26	6	25	11	9	7	97	5208	11	3	93	5	2	97	14	38	417	33
101-115	10	8	35	10	32	23	14	8	118	8575	12	4	106	1	3	125	18	60	338	32
101-116	6	7	28	6	27	13	9	7	91	7032	8	2	87	5	2	106	13	33	308	33
101-117	9	5	29	8	27	21	9	7	115	8496	14	0	92	8	2	118	16	55	241	32
101-118	15	7	33	13	31	36	13	8	138	9415	17	4	92	11	6	128	22	97	288	33

A.3 Results TGA and CS anayses

Sample code	TC (%)	TIC (%)	Sulfur (%)	Weight loss 105-450° C (%)	Weight loss 450-550° C (%)	Weight loss 550-800° C (%)	Weight loss 800-1000° C (%)
101-95	0.11	0	0.373	0.913	0.423	0.252	0.276
101-96	0.59	0	1.48	3.125	1.183	0.74	0.54
101-97	1.45	0.51	0.77	1.679	1.046	2.938	0.21
101-98	3.55	2.02	0.864	2.16	1.85	9.112	0.334
101-99	0.78	0.16	0.91	1.533	0.871	1.028	0.476
101-100	2.9	1.73	0.73	2.479	2.501	8.552	0.334
101-101	3.83	2.58	0.844	2.193	2.345	11.25	0.265
101-102	2.09	1.33	0.339	2.235	1.857	6.029	0.298
101-103	0.82	0.38	0.169	1.612	0.928	2.008	0.166
101-104	0.41	0	0.665	2.764	0.918	0.867	0.454
101-105	0.4	0	1.88	3.035	0.716	1.617	0.638
101-106	0.27	0	0.442	2.17	0.601	0.558	0.301
101-107	0.33	0	0.654	2.137	0.815	0.666	0.304
101-107d	0.31	0	0.674	2.085	0.844	0.644	0.315
101-108	0.26	0	0.767	1.97	0.669	0.532	0.327
101-109	0.25	0	0.668	1.887	0.598	0.518	0.274
101-110	0.42	0	0.938	3.204	1.199	0.955	0.757
101-111	0.37	0	1.12	3.017	0.844	1.223	0.758
101-112	0.51	0	1.85	3.927	2.275	1.409	1.024
101-113	0.92	0	4.31	3.886	2.029	1.537	1.514
101-114	0.21	0	0.498	1.647	0.441	0.53	0.251
101-115	0.41	0	1.34	2.514	0.906	0.974	0.494
101-116	0.24	0	0.714	1.795	0.397	0.805	0.431
101-117	0.43	0	1.1	3.362	0.981	1.513	0.785
101-118	0.7	0	2.43	2.791	1.304	1.062	0.712

A.4 ICP-OES after HF-digestion

Sample Id	Al (ppm)	As (ppm)	Be (ppm)	Ca (ppm)	Ce (ppm)	Co (ppm)	Cu (ppm)	Fe (ppm)	K (ppm)	Li (ppm)	Mg (ppm)
101-95	36334	20.4	1.31	2033	36.2	12.1	44.1	20213	23343	20.2	4030
101-96	56447	23.6	2.05	1292	52.8	24.5	67.3	37532	23866	37.8	8870
101-97	35887	8.9	1.98	29734	41	13	43.8	37340	22108	25.2	6379
101-98	41552	7.6	1.6	107815	44.3	14.9	45.8	32410	19603	35.3	7286
101-99	41397	14.8	2.21	22387	48.3	17.2	43.2	43688	24132	29.4	7504
101-100	53244	11.2	1.67	89895	48	13.8	42.6	32249	20542	43.1	9615
101-101	58961	7.9	1.58	120083	44.2	13.5	35.5	29894	18274	47.4	10987
101-102	58561	10.6	1.84	58544	42.8	15.8	38.2	35318	21863	47.4	10540
101-103	42445	12.7	2.06	25882	54.6	14.2	31.8	38255	23462	29.1	8076
101-104	64136	20.7	1.99	3298	56.1	16.5	36.1	37496	24294	48.1	10279
101-105	48084	19.5	1.54	3921	32.6	9.9	22.2	42305	22338	33.3	6559
101-106	41948	17.7	2.7	3487	53.2	12.1	28.6	53029	29366	28	8650
101-107	49797	15.4	2.73	4868	57.5	12.7	28.6	52852	28310	37.4	10029
101-107duplo	44163	12.1	2.5	3781	54.7	12.2	20.9	48045	25821	33.3	8969
101-108	39859	16.8	2.85	2395	62.1	13.9	36.2	52624	29384	32.5	8838
101-109	40222	19.3	2.72	2948	61.8	12.2	21.2	50583	29158	28.2	8665
101-110	60858	22.3	2.55	2189	61.3	13.9	24.3	44720	26649	48.3	10718
101-111	51831	19.8	2.5	3217	60.8	12.4	19.6	46985	26440	39.5	9278
101-112	86784	46.1	2.99	1400	78.8	20.7	44.1	49551	27585	71.8	13436
101-113	80191	49.4	2.84	1149	79.1	19.3	45.5	50458	26216	71.3	12424
101-114	34814	12	2.22	1760	51.2	9.1	19.6	39019	26061	25.6	6162
101-115	55590	30	2.64	2020	65.7	12.7	34.6	50114	29004	46.3	8952
101-116	33224	16.2	2.12	1702	50.6	8.6	24.6	34086	23543	24.8	5863
101-117	30671	21.2	2	1378	36.9	7.9	21.3	41282	24886	21.7	5467
101-118	66005	24.8	2.52	1470	61.2	14.6	37.9	44531	27096	58.7	9600

Sample Id	Mn (ppm)	Na (ppm)	Ni (ppm)	P (ppm)	S (ppm)	Sc (ppm)	Sr (ppm)	Ti (ppm)	V (ppm)	Y (ppm)	Zn (ppm)
101-95	107	9657	21.1	232	2903	7	111	3066	74	13.5	66
101-96	148	9057	49.9	254	8920	13.6	84	4647	145	19.4	114
101-97	145.2	6675	17.7	540	3078	8.8	237	3187	76	15.4	41
101-98	201.7	6734	22.6	437	4142	9.4	655	3169	83	16.1	57
101-99	122.9	7022	28.2	358	6207	10	212	3351	82	13.1	44
101-100	200.1	5934	27.9	380	3696	11.2	498	3800	105	14.7	62
101-101	228.7	5014	28	215	4991	11.6	634	3462	117	13.6	60
101-102	142.9	5694	30.4	325	4176	12.1	404	3828	116	13.7	71
101-103	125.8	6109	21.8	377	2096	10.1	243	3605	111	14.9	49
101-104	135.7	6842	34.8	230	5789	13.3	136	5124	146	17.1	83
101-105	105.6	7002	28.5	180	17353	9.2	162	3695	95	10.8	45
101-106	98.7	5543	21.8	288	5147	10.9	138	3248	147	13.5	52
101-107	84.1	4493	20.3	254	7415	12.7	132	3375	154	13.6	55
101-107duplo	76.8	3935	18.4	259	6496	11.5	117	2970	138	12	49
101-108	73.3	4461	19.8	268	4685	11.5	110	2362	143	12.6	51
101-109	78.1	4552	22.5	337	4838	11.2	134	2691	143	14.1	47
101-110	91.5	4392	29.4	240	8609	14.1	113	3895	171	16.8	67
101-111	88.2	4199	26.4	275	9365	12.7	122	3320	152	15.2	62
101-112	101.3	4259	47.7	185	16173	18.7	109	5205	252	22.5	96
101-113	103.6	4294	53.7	168	22641	18	100	5388	253	22.2	84
101-114	73.9	4358	15.2	305	4554	9.6	107	2403	120	11.2	39
101-115	94.6	4800	29.1	234	11565	13.6	111	3528	175	15.4	70
101-116	56.4	3612	15.3	138	4562	9.3	75	1962	123	9.5	37
101-117	49.2	3829	14.7	216	6965	8.9	99	1815	113	7.9	45
101-118	107	5037	40.7	182	15351	15	104	4404	172	17.6	92

A.5 ICP-MS after HF-digestion

Sample Id	Sc 45 (ppm)	V 51 (ppm)	Cr 52 (ppm)	Mn 55 (ppm)	Fe 57 (ppm)	Co 59 (ppm)	Ni 60 (ppm)	Cu 63 (ppm)	Zn 66 (ppm)	As 75 (ppm)
101-95	7.9	80	74	111	21356	12.7	18.4	6.3	61.8	17
101-96	15.7	158	123	156	39210	26.8	48	19.4	107.3	30.4
101-97	10.4	81	106	152	38889	14	18.3	6.8	38.6	11.3
101-98	10.9	90	97	213	34588	16.8	23.8	10.6	55.7	14
101-99	11.7	88	122	128	44229	18.8	26.8	7.9	42.3	13.3
101-100	13	114	101	210	34110	15.3	28.2	12.4	61.2	12.3
101-101	14.3	131	96	251	33041	16.4	31.2	12.5	62.3	13.6
101-102	14	126	114	149	37264	18.3	30.9	13.2	71.9	12.3
101-103	11.4	116	129	129	38441	14.7	19.7	8.2	46.9	12.2
101-104	14.7	153	133	137	37744	15.9	31.9	14.4	78.9	22.1
101-105	10.8	100	94	110	41044	11.1	27.1	11	42.6	21.5
101-106	12.4	156	163	102	53212	13.7	19.4	7.9	48.1	16.7
101-107	13.8	161	149	86	52127	13.5	19.7	9.5	50.5	17.4
101-107duplo	13.5	154	141	84	50728	13	18.3	8.8	49	17.5
101-108	13.6	162	157	81	55958	15	19.1	7.4	47	21.9
101-109	13.4	158	158	86	53031	13.7	22	6.2	46.2	21
101-110	16.1	189	140	97	46355	15.5	29.1	10.6	64.1	26.7
101-111	15.1	169	142	96	48986	15.2	26.2	10.2	62.4	22.2
101-112	21.2	282	159	109	51798	21.1	45.7	31.3	92.5	49.7
101-113	21.5	286	166	112	54237	21.5	50.7	33	82.6	57
101-114	11.7	139	125	83	43535	10.5	14.8	6.3	38.3	18
101-115	16.5	198	150	102	53650	14.9	28.9	12	62.3	33.5
101-116	10.7	138	123	61	36607	8.6	13.9	6	34.7	19.9
101-117	10.2	126	106	54	43758	9	13.3	7.3	42.9	20.8
101-118	17.7	192	147	116	47366	17.1	40.1	23.9	88.2	32.9

Sample Id	Li 7 (ppm)	Be 9 (ppb)	Se 82 (ppb)	Rb 85 (ppm)	Sr 88 (ppm)	Y 89 (ppm)	Zr 90 (ppm)	Nb 93 (ppm)	Mo 98 (ppb)	Ag 107 (ppb)	Cd 111 (ppm)	Sn 118 (ppb)
101-95	18.6	1269	595	68	110	12.7	134	11.7	210	359	140	3683
101-96	38	2062	1169	100	83	18.2	136	21.3	691	415	157	13061
101-97	24.1	2025	817	75	238	14.4	155	11.9	587	387	133	2373
101-98	34	1669	1295	73	676	15.6	127	13.3	723	353	198	4542
101-99	28.9	2232	890	88	208	12.3	148	12.3	586	356	123	1909
101-100	43.7	1754	987	96	512	14.2	116	17.4	390	342	130	3134
101-101	49.6	1705	1135	102	681	13.7	94	19.2	422	259	131	4929
101-102	49.2	1941	1107	105	417	13.2	120	17.8	415	322	135	5393
101-103	29	2060	800	91	238	13.7	125	13.3	259	345	123	3146
101-104	50.2	1958	1081	112	134	15.8	184	20.9	3307	429	171	6032
101-105	36.2	1556	755	87	159	10	115	15.3	6740	280	123	1565
101-106	29.3	2826	895	114	139	12.7	173	13.6	516	394	192	4739
101-107	39.1	2752	898	123	130	12.4	119	16.4	752	331	89	4169
101-107duplo	36.1	2620	939	113	118	11.3	111	14.3	726	321	91	2717
101-108	31.4	3128	955	110	104	10.9	89	12.4	659	272	156	2427
101-109	31	2902	766	119	136	13.3	137	11.6	584	383	162	4900
101-110	53.3	2659	962	133	114	15.8	129	19.2	1297	354	153	9374
101-111	44.9	2753	957	121	124	14.9	144	15.8	1629	338	140	3570
101-112	80.4	3182	1488	169	110	21	156	27.1	1501	387	179	4177
101-113	80	3005	1732	157	105	21.4	140	28.3	4790	372	168	5401
101-114	27.5	2513	625	99	113	10.8	129	10.5	732	346	161	1440
101-115	50.4	2910	1041	128	113	14.7	123	15.9	1941	329	187	2456
101-116	25.8	2227	599	89	78	9	78	8.9	718	215	140	1659
101-117	23	2113	665	82	102	7.5	69	7.4	1149	207	147	951
101-118	65.3	2685	1479	132	107	16.6	123	20.4	4557	329	245	1944

Sample Id	Sb 121 (ppb)	Cs 133 (ppb)	Ba 137 (ppm)	La 139 (ppm)	Ce 140 (ppm)	Pr 141 (ppb)	Nd 146 (ppm)	Sm 147 (ppb)	Eu 151 (ppb)	Gd 157 (ppb)	Tb 159 (ppb)	Dy 163 (ppb)
101-95	385	2148	519	18.2	40.5	4530	17.7	3636	889	3255	473	2699
101-96	1198	4993	369	27.9	67.9	7503	29.6	6022	1389	5273	750	4206
101-97	413	2887	325	23.3	48	5680	22.4	4376	993	3954	528	2926
101-98	536	3651	279	25	50.3	6018	23.9	4693	1039	4186	572	3184
101-99	477	3168	344	25.1	58.7	6342	24.8	4815	1017	4063	531	2778
101-100	458	5219	295	27.3	61	6690	25.9	5106	1103	4330	590	3209
101-101	437	6496	199	26.8	58.7	6220	23.7	4559	999	3838	527	2951
101-102	435	5882	304	24.9	55.3	5888	22.6	4371	957	3727	506	2835
101-103	365	3736	344	26.3	63.2	6625	25.9	5060	1073	4250	567	3035
101-104	625	5744	403	29.2	69.6	7278	27.9	5323	1158	4503	611	3366
101-105	469	3541	467	19.6	45	4663	17.8	3390	738	2823	384	2130
101-106	517	3873	369	25.6	63.4	6359	24.5	4672	984	3871	506	2745
101-107	435	5222	316	26.7	66.8	6449	24.7	4636	999	3794	494	2646
101-	740	4781	300	26.3	66.4	6277	23.8	4437	919	3584	459	2423
101-108	890	4142	329	27.5	70.8	6931	26.4	4944	1002	3928	485	2449
101-109	523	4129	340	29.5	71.7	7038	27.1	5125	1055	4194	541	2837
101-110	650	7081	322	29.7	74.5	7492	28.9	5490	1168	4591	607	3316
101-111	516	5749	320	30.1	73.9	7421	28.5	5341	1129	4447	582	3124
101-112	805	11008	299	40.7	97.4	10206	39.2	7414	1608	6137	821	4492
101-113	877	9969	290	39.7	98.6	10377	40	7542	1625	6163	830	4538
101-114	404	3231	362	26.5	63.1	6081	23	4276	910	3481	442	2342
101-115	544	5898	364	31.4	78.9	7997	30.8	5838	1242	4747	610	3247
101-116	419	3007	320	20.3	56.3	5487	21.2	3939	868	3177	398	2015
101-117	407	2620	347	17.1	39.8	4236	16.4	3158	728	2529	320	1671
101-118	680	7365	353	31.4	76.2	8052	31	5924	1297	4896	658	3638

Sample Id	Ho 165 (ppb)	Er 166 (ppb)	Tm 169 (ppb)	Yb 172 (ppb)	Lu 175 (ppb)	Hf 178 (ppb)	Ta 181 (ppb)	Re 185 (ppb)	Tl 205 (ppb)	Pb 207 (ppm)	Th 232 (ppb)	U 238 (ppb)
101-95	511	1497	214	1434	216	3816	758	4.1	477	13	3991	1492
101-96	778	2209	310	2064	306	3800	1656	5.9	1678	12.1	7284	2644
101-97	552	1575	218	1443	217	4046	751	5.2	783	10	4619	1736
101-98	602	1702	237	1561	231	3582	908	7.7	591	9.6	5480	2033
101-99	495	1377	189	1261	186	3757	840	4	448	10.9	5389	1453
101-100	598	1671	233	1560	228	3294	1223	4.5	418	12.3	7176	1656
101-101	557	1615	228	1531	223	2624	1317	6.1	401	12.7	7384	1720
101-102	532	1539	221	1465	220	3327	1218	6.4	407	13.4	7349	1579
101-103	546	1537	212	1383	207	3583	851	7.4	322	11.1	6631	1653
101-104	627	1834	260	1737	268	4599	1349	5.2	374	14.2	8182	2195
101-105	405	1194	173	1169	178	3018	1094	3.8	298	15.4	5453	1453
101-106	499	1439	205	1379	207	4298	962	10.4	360	11.5	6361	2028
101-107	489	1395	195	1296	193	3253	886	3.9	319	12.3	6811	2141
101-	443	1256	176	1168	174	3042	984	3.4	1488	11.4	6494	1966
101-108	430	1198	162	1042	152	2418	1022	9	1701	10.1	5742	1944
101-109	515	1455	201	1337	200	3783	736	6	865	11.2	6663	2043
101-110	608	1761	247	1634	243	3575	1340	5.3	689	13.4	7213	2266
101-111	582	1657	234	1558	232	3675	1061	5.2	480	14.1	7473	1911
101-112	839	2413	339	2221	331	3845	1829	9.8	569	17.4	11426	3333
101-113	850	2429	341	2241	328	3870	2013	12.7	580	21.5	11869	4050
101-114	424	1208	170	1140	173	3509	666	7.6	384	11.1	5778	1843
101-115	589	1669	231	1511	223	3429	1034	8.4	385	13.8	7490	3180
101-116	354	980	132	844	123	2151	570	10.6	295	8.1	3513	1999
101-117	300	835	114	747	110	1913	474	6	267	11.3	3228	1583
101-118	667	1927	267	1772	260	3409	1379	14.8	377	14.7	9195	5190

Appendix B

Results groundwater

B.1 Field and carbon parameters

Table 5-1: Field parameters, total inorganic carbon and methane concentrations for the groundwater samples

Sample code	Well	Filter	Location	Sample date	Top of filter (mbs)	Bottom of filter (mbs)	Groundwater head (mbs)	pH (-)	Temperature (°C)	EC (µS/cm)	O_2 (mg/l)	HCO_3 (mg/l)	Radon (Bq/l)	TIC (mg/l)	CH_4 (mg/l)
WV01	B48G0100	1	Ovezande	3-9-2024	5.6	6.6	3.36	7.27	14	1360	0.25	663.68	3.4	153	0.00
WV02	B48G0100	4	Ovezande	3-9-2024	19.7	20.7	3.35	7.96	13	1838	0.26	678.32	2.2	144	0.02
WV03	B48G0100	5	Ovezande	3-9-2024	30.5	31.5	3.37	7.46	13.3	42400	0.31	963.8		182	0.01
WV04	B48G0100	6	Ovezande	3-9-2024	42.7	43.7	3.66	7.2	13.1	47600	0.26	756.4		155	0.01
WV05	B48G0204	1	Ovezande	4-9-2024	90.9	148.2	-0.045	8.6	13.5	2290	0.25	610	10.0	101	0.01
WV06	B48E0224	1	s-Heer Arendskerke	4-9-2024	127.5	132.5	-0.05	7.89	14	7230	0.3	750.3	8.9	152	0.01
WV07	B55A0341/B55A0340	1	Hulst	4-9-2024	153.8	207.15	7.48	8	16.1	9100	0.23	780.8	4.5	143	0.01
WV08	B55A0340/B550341	1	Hulst	5-9-2024	75.15	102.15	6.35	8.85	14.6	1532	0.4	927.2	10.3	150	0.05
WV09	B48C0196	1	Groede	10-9-2024	117	187	2.41	7.99	15.7	7350	0.25	866.2	3.8	182	0.01
WV10	B54E0238	1	Sluiskil	10-9-2024	2.6	3.6	1.87	6.54	16.2	26600	2.47	750.3		184	0.04
WV11	B54E0238	2	Sluiskil	10-9-2024	6.5	7.5	1.92	6.44	13.3	31800	0.18	847.9		180	0.05
WV12	B54E0238	3	Sluiskil	10-9-2024	21.9	22.9	1.9	6.58	12.5	34900	0.2	811.3		164	0.08
WV13	B54B0093	1	Pyramide	10-9-2024	18.4	19.4	2.27	8.48	12.5	3220	0.3	939.4		198	0.07
WV14	B48H0291	1	Kloosterzande	11-9-2024	93.9	150	1.84	8.32	14	4220	0.25	658.8	10.6	134	0.01
WV15	B54F0093	1	Axel	11-9-2024	77	100	2.04	8.78	13.1	2390	0.4	750.3	10.7	141	0.05

B.2 ICP-MS

Table 5-2: ICP-MS results for the groundwater samples. LOQ = Limit of Quantification. See table Table 3.1 for the link between the sample names and the locations and filter depths.

	Sc	V	Cr	Mn	Fe	Co	Ni	Cu	Zn	As	Li	Be	Se	Rb	Sr	Y	Zr	Nb
	µg/l	µg/l	µg/l	µg/l	µg/l	µg/l	µg/l	µg/l	µg/l	µg/l	µg/l	µg/l	µg/l	µg/l	µg/l	µg/l	µg/l	µg/l
LOQ	0.06	0.03	0.02	0.04	1.3	0.009	0.04	0.02	0.15	0.2	0.1	0.021	0.1	0.02	0.02	0.015	0.08	0.2
Sample																		
WV01	0.24	0.17	0.27	995.6	14454.0	1.394	2.20	0.48	50.75	3.3	50.1	<0.021	1.3	3.5	1167.8	0.051	0.91	<0.2
WV02	0.07	0.62	0.21	223.0	4092.4	0.270	0.73	0.32	6.98	8.4	39.6	<0.021	3.7	14.3	1253.1	0.032	0.73	<0.2
WV03	0.40	2.63	0.25	955.2	11180.7	0.833	0.61	0.42	19.15	5.7	161.2	<0.021	127.7	65.5	5737.8	0.095	1.75	<0.2
WV04	0.23	2.21	0.53	337.2	21858.8	4.539	2.92	0.60	41.60	23.7	174.1	<0.021	131.5	100.0	6206.7	0.085	2.09	<0.2
WV05	0.11	<0.03	0.06	8.8	19.0	0.955	1.04	0.34	<0.15	<0.2	82.2	<0.021	3.2	4.8	233.3	<0.015	0.08	<0.2
WV06	0.08	0.23	0.09	29.6	8.5	0.093	0.06	0.20	0.33	2.0	248.3	<0.021	12.0	11.0	981.8	0.018	0.12	<0.2
WV07	0.16	0.28	0.18	24.9	198.0	0.216	0.31	0.26	2.32	<0.2	406.0	<0.021	16.9	9.3	1583.6	0.028	0.10	<0.2
WV08	0.18	4.72	0.30	238.8	121.3	0.546	0.61	0.18	1.72	16.5	55.8	0.022	0.9	2.8	88.0	2.665	0.48	<0.2
WV09	0.06	0.39	0.30	11.3	37.6	0.104	0.32	0.33	0.54	0.3	264.4	<0.021	12.4	6.6	912.4	0.041	0.55	<0.2
WV10	0.65	4.42	1.04	5011.6	15424.3	13.602	21.22	0.22	8.78	65.7	108.8	<0.021	74.4	8.1	10972.4	0.182	0.75	<0.2
WV11	0.90	1.78	1.08	5885.7	71427.1	0.990	1.20	0.38	12.18	5.4	123.8	<0.021	91.9	1.5	13870.0	0.173	0.37	<0.2
WV12	0.51	1.24	1.33	2747.5	116196.1	4.780	2.12	0.77	113.03	7.9	142.4	0.023	97.7	36.4	9662.9	0.162	0.63	<0.2
WV13	0.33	45.73	5.22	93.5	1797.2	0.904	1.71	1.36	1.96	11.6	17.2	0.496	7.5	6.0	118.5	1.192	18.78	<0.2
WV14	<0.06	0.10	0.12	16.7	474.2	0.057	0.25	0.33	0.59	1.9	105.9	<0.021	8.6	8.5	695.6	0.074	0.11	<0.2
WV15	<0.06	0.23	0.28	104.2	209.8	0.129	0.15	0.32	<0.15	24.9	68.9	<0.021	3.9	3.3	106.5	0.031	0.35	<0.2

	Mo	Ag	Cd	Sn	Sb	Cs	Ba	La	Ce	Pr	Nd	Sm	Eu	Gd	Tb	Dy	Ho	Er
	µg/l	µg/l	µg/l	µg/l	µg/l	µg/l	µg/l	µg/l	µg/l	µg/l	µg/l	µg/l	µg/l	µg/l	µg/l	µg/l	µg/l	µg/l
LOQ	0.03	0.06	0.005	0.10	0.06	0.003	0.006	0.004	0.004	0.0003	0.0003	0.0002	0.0002	0.0003	0.001	0.0010	0.001	0.001
Sample																		
WV01	0.14	<0.06	0.025	<0.10	0.19	0.021	15.9	0.021	0.052	0.006	0.035	0.0097	0.0023	0.006	0.001	0.0057	<0.001	0.004
WV02	0.69	<0.06	<0.005	<0.10	0.17	0.021	9.2	0.009	0.018	0.002	0.009	0.0024	0.0011	0.002	<0.001	0.0021	<0.001	0.002
WV03	1.87	<0.06	<0.005	<0.10	1.55	0.076	55.5	0.760	0.047	0.005	0.022	0.0054	0.0031	0.007	0.002	0.0058	<0.001	0.006
WV04	1.76	<0.06	<0.005	0.17	2.04	0.289	82.9	0.030	0.036	0.006	0.016	0.0045	0.0046	0.004	0.002	0.0050	<0.001	0.005
WV05	2.63	<0.06	<0.005	<0.10	0.11	<0.003	2.6	<0.004	0.008	0.001	0.004	0.0011	0.0007	0.002	<0.001	0.0014	<0.001	0.002
WV06	9.12	<0.06	<0.005	<0.10	0.20	0.008	13.3	<0.004	<0.004	<0.0003	0.001	0.0004	0.0007	0.001	<0.001	0.0011	<0.001	<0.001
WV07	11.50	<0.06	<0.005	<0.10	0.10	0.020	7.7	0.009	0.017	0.002	0.010	0.0038	0.0012	<0.0003	<0.001	0.0039	<0.001	0.002
WV08	2.86	<0.06	<0.005	<0.10	0.09	0.029	36.9	7.050	19.637	1.774	7.128	1.3360	0.3079	1.116	0.145	0.6756	0.108	0.261
WV09	26.28	<0.06	<0.005	<0.10	0.19	0.013	4.7	0.010	0.012	0.001	0.005	0.0009	0.0008	0.001	<0.001	0.0015	<0.001	0.002
WV10	2.84	<0.06	<0.005	<0.10	1.83	0.011	867.2	0.057	0.082	0.009	0.040	0.0126	0.0398	0.012	0.002	0.0127	0.003	0.009
WV11	0.33	<0.06	<0.005	<0.10	1.17	0.038	852.5	0.080	0.111	0.011	0.056	0.0128	0.0349	0.011	0.003	0.0096	0.003	0.008
WV12	0.48	<0.06	<0.005	<0.10	1.69	0.184	453.6	0.312	0.127	0.013	0.060	0.0150	0.0206	0.015	0.002	0.0100	0.002	0.008
WV13	1.97	<0.06	<0.005	<0.10	0.35	0.038	24.5	0.999	2.190	0.225	0.953	0.2134	0.0575	0.221	0.033	0.2015	0.042	0.129
WV14	11.14	<0.06	0.008	<0.10	0.40	0.009	17.3	0.006	0.015	0.002	0.010	0.0032	0.0014	0.004	0.001	0.0056	<0.001	0.005
WV15	26.91	<0.06	0.018	<0.10	0.39	0.015	27.7	0.009	0.012	0.002	0.007	0.0020	0.0015	0.002	<0.001	0.0029	<0.001	0.002

	Tm	Yb	Lu	Hf	Ta	W	Re	Hg	Tl	Pb	Th	U
	µg/l	µg/l	µg/l	µg/l	µg/l	µg/l	µg/l	µg/l	µg/l	µg/l	µg/l	µg/l
LOQ	0.0008	0.0006	0.0006	0.004	0.06	0.6	0.0005	0.08	0.97	0.004	0.001	0.0004
Sample												
WV01	<0.0008	0.0034	0.0009	0.055	<0.06	<0.6	0.0009	1.30	0.98	0.015	0.006	0.0205
WV02	<0.0008	0.0022	<0.0006	0.049	<0.06	<0.6	0.0015	2.02	1.47	0.046	0.007	0.0276
WV03	<0.0008	0.0035	<0.0006	0.103	<0.06	<0.6	0.0013	3.80	5.54	0.120	0.012	0.0925
WV04	<0.0008	0.0046	0.0007	0.099	0.09	<0.6	0.0024	7.76	16.29	0.212	0.021	0.0832
WV05	<0.0008	0.0009	<0.0006	<0.004	<0.06	<0.6	<0.0005	1.53	<0.97	0.008	0.012	0.0339
WV06	<0.0008	0.0015	<0.0006	<0.004	<0.06	<0.6	<0.0005	2.33	<0.97	<0.004	0.026	0.1645
WV07	<0.0008	0.0020	<0.0006	<0.004	<0.06	<0.6	<0.0005	2.38	<0.97	0.024	0.089	0.0354
WV08	0.031	0.1602	0.0225	0.013	<0.06	<0.6	0.0071	1.10	<0.97	0.645	3.476	0.6736
WV09	<0.0008	0.0012	<0.0006	0.011	<0.06	<0.6	<0.0005	1.52	<0.97	<0.004	0.006	0.0361
WV10	0.0020	0.0098	0.0025	0.011	<0.06	<0.6	0.0054	1.37	1.44	0.088	0.006	0.1326
WV11	0.0010	0.0087	0.0014	0.008	<0.06	<0.6	0.0014	2.69	1.74	0.062	0.008	0.0806
WV12	0.0010	0.0090	0.0010	0.010	<0.06	<0.6	0.0011	4.02	3.06	0.134	0.021	0.1142
WV13	0.0194	0.1306	0.0229	0.231	<0.06	<0.6	0.0043	4.50	3.25	0.405	0.438	0.2232
WV14	<0.0008	0.0042	0.0008	0.006	<0.06	<0.6	<0.0005	1.07	<0.97	0.023	<0.001	0.0849
WV15	<0.0008	0.0020	<0.0006	0.021	<0.06	<0.6	<0.0005	1.31	1.17	0.009	0.002	0.0745

B.3 ICP-OES

	Al	B	Ba	Be	Ca	Cd	Co	Cr	Cu	Fe	K	Li	Mg	Mn	Mo	Na	Ni	P
	µg/l	mg/l	µg/l	µg/l	mg/l	µg/l	µg/l	µg/l	µg/l	µg/l	mg/l	µg/l	mg/l	µg/l	µg/l	mg/l	µg/l	mg/l
LOQ	19	0.05	1.2	1.1	0.06	8.3	10.7	7.7	63.8	61	0.2	3.5	0.02	1.4	33.5	0.1	26.5	0.1
Sample																		
WV01	44.6	0.32	17.0	<1.1	214.5	<8.3	<10.7	<7.7	<63.8	14054	10.6	47.5	25.7	1007.9	<33.5	37.1	<26.5	0.3
WV02	31.9	1.03	10.0	<1.1	128.0	<8.3	<10.7	<7.7	<63.8	4350	64.8	37.7	85.2	234.4	<33.5	123.1	<26.5	1.7
WV03	55.0	3.59	47.0	<1.1	350.2	<8.3	<10.7	<7.7	<63.8	8757	321.4	181.4	>>	763.1	<33.5	>>	<26.5	0.3
WV04	56.1	3.67	69.0	<1.1	354.5	<8.3	<10.7	<7.7	<63.8	16684	359.3	210.7	>>	271.9	<33.5	4714.5	<26.5	0.5
WV05	<19	3.05	4.7	<1.1	9.6	<8.3	<10.7	<7.7	<63.8	213	23.1	80.6	10.3	11.6	<33.5	471.6	<26.5	<0.1
WV06	<19	5.52	18.6	<1.1	27.2	<8.3	<10.7	<7.7	<63.8	213	44.6	236.5	35.0	30.3	<33.5	1408.3	<26.5	<0.1
WV07	<19	6.39	7.9	<1.1	29.3	<8.3	<10.7	<7.7	<63.8	374	35.8	404.9	24.2	24.8	<33.5	1769.7	<26.5	<0.1
WV08	<19	5.77	40.0	<1.1	3.8	<8.3	<10.7	<7.7	<63.8	324	14.2	52.0	3.3	249.3	<33.5	358.2	<26.5	0.6
WV09	<19	5.11	7.0	<1.1	19.1	<8.3	<10.7	<7.7	<63.8	208	31.3	264.1	18.6	11.6	<33.5	1521.9	<26.5	<0.1
WV10	117.1	0.85	758.9	<1.1	>>	<8.3	<10.7	<7.7	<63.8	11991	141.4	121.2	545.8	4108.2	<33.5	2378.2	<26.5	0.7
WV11	104.0	0.44	723.2	<1.1	>>	<8.3	<10.7	<7.7	<63.8	52755	105.8	141.0	733.9	4652.2	<33.5	2681.9	<26.5	0.3
WV12	89.9	0.24	383.4	<1.1	>>	<8.3	<10.7	<7.7	<63.8	89455	60.1	160.4	707.3	2215.1	<33.5	3733.5	<26.5	0.1
WV13	81.9	3.13	27.1	<1.1	9.5	<8.3	<10.7	11.8	<63.8	2265	34.2	15.6	17.9	98.4	<33.5	734.7	<26.5	11.8
WV14	<19	5.63	17.3	<1.1	21.6	<8.3	<10.7	<7.7	<63.8	616	35.6	159.4	25.2	17.0	<33.5	855.1	<26.5	<0.1
WV15	<19	4.58	41.4	<1.1	4.3	<8.3	<10.7	<7.7	<63.8	384	17.0	74.1	3.8	110.0	<33.5	542.0	<26.5	0.4

	Pb	S	Sc	Si	Sr	Ti	V	Y	Zn	Zr
	µg/l	mg/l	µg/l	mg/l	mg/l	µg/l	µg/l	µg/l	µg/l	µg/l
LOQ	82	0.4	0.9	0.06	0.001	1.4	7.4	1.5	12.2	3.8
Sample										
WV01	<82	21.0	<0.9	37.5	1.4	<1.4	<7.4	<1.5	47.8	<3.8
WV02	<82	64.9	<0.9	13.2	1.5	<1.4	<7.4	<1.5	<12.2	<3.8
WV03	<82	622.3	<0.9	6.0	5.5	<1.4	<7.4	<1.5	15.8	<3.8
WV04	<82	611.3	<0.9	6.7	5.9	<1.4	<7.4	<1.5	36.1	<3.8
WV05	<82	9.0	<0.9	6.5	0.3	<1.4	<7.4	<1.5	<12.2	<3.8
WV06	<82	100.4	<0.9	7.1	1.1	<1.4	<7.4	<1.5	<12.2	<3.8
WV07	<82	49.8	<0.9	16.8	1.8	<1.4	<7.4	<1.5	<12.2	<3.8
WV08	<82	2.5	<0.9	4.7	0.1	4.4	<7.4	3.2	<12.2	<3.8
WV09	<82	103.3	<0.9	17.4	1.1	<1.4	<7.4	<1.5	<12.2	<3.8
WV10	145	118.9	<0.9	9.8	10.9	<1.4	<7.4	<1.5	<12.2	<3.8
WV11	147	157.3	<0.9	9.9	13.4	<1.4	<7.4	<1.5	<12.2	<3.8
WV12	103	236.5	<0.9	12.9	9.3	<1.4	<7.4	<1.5	91.7	<3.8
WV13	<82	43.7	<0.9	10.2	0.1	89.7	51.0	<1.5	<12.2	28.4
WV14	<82	55.1	<0.9	5.5	0.8	<1.4	<7.4	<1.5	<12.2	<3.8
WV15	<82	7.5	<0.9	7.8	0.1	<1.4	<7.4	<1.5	<12.2	<3.8

B.4 IC

	F	Cl	NO_2	Br	NO_3	PO_4	SO_4
	mg/l	mg/l	mg/l	mg/l	mg/l	mg/l	mg/l
LOQ	0.027	6	0.006	0.18	0.15	0.24	1.2
Sample							
WV01	1.33	77	<0.006	0.40	<0.15	<0.24	62.8
WV02	0.45	162	<0.006	0.64	<0.15	0.97	189.0
WV03	0.84	>>	<0.006	55.75	<0.15	<0.24	1984.0
WV04	0.08	>>	<0.006	65.34	<0.15	<0.24	1974.4
WV05	0.69	496	<0.006	1.58	<0.15	0.32	26.2
WV06	0.52	1894	<0.006	6.31	<0.15	0.32	308.4
WV07	0.99	2605	<0.006	9.14	<0.15	<0.24	148.1
WV08	2.18	141	<0.006	0.48	<0.15	1.83	6.8
WV09	0.67	1898	<0.006	6.45	<0.15	0.29	313.7
WV10	0.14	>>	<0.006	36.07	<0.15	0.43	396.4
WV11	0.05	>>	<0.006	44.01	<0.15	0.27	540.3
WV12	0.05	>>	<0.006	46.35	<0.15	<0.24	806.5
WV13	3.05	555	<0.006	1.95	<0.15	34.71	122.5
WV14	0.82	1017	<0.006	3.24	<0.15	<0.24	162.6
WV15	1.24	462	<0.006	1.43	<0.15	1.43	21.7

Energy & Materials Transition

Princetonlaan 6
3584 CB Utrecht
www.tno.nl

TNO innovation for life